

Air–sea CO₂ fluxes in the East China Sea

X.-H. Guo et al.

Air–sea CO₂ fluxes in the East China Sea based on multiple-year underway observations

X.-H. Guo¹, W.-D. Zhai^{1,2}, M.-H. Dai¹, C. Zhang¹, Y. Bai³, Y. Xu¹, Q. Li¹, and G.-Z. Wang¹

¹State Key Laboratory of Marine Environmental Science, Xiamen University, Xiamen 361102, China

²National Environmental Monitoring Center, Dalian 116023, China

³State Key Laboratory of Satellite Ocean Environment Dynamics, Second Institute of Oceanography, State Oceanic Administration, Hangzhou 310012, China

Received: 22 February 2015 – Accepted: 6 March 2015 – Published: 1 April 2015

Correspondence to: M.-H. Dai (mdai@xmu.edu.cn)

Published by Copernicus Publications on behalf of the European Geosciences Union.

Title Page

Abstract

Introduction

Conclusions

References

Tables

Figures



Back

Close

Full Screen / Esc

Printer-friendly Version

Interactive Discussion



Abstract

This study reports thus far a most comprehensive dataset of surface seawater $p\text{CO}_2$ (partial pressure of CO_2) and the associated air–sea CO_2 fluxes in a major ocean margin, the East China Sea (ECS) based on 24 surveys conducted in 2006 to 2011.

5 We showed highly dynamic spatial variability of sea surface $p\text{CO}_2$ in the ECS except in winter when it ranged in a narrow band of 330 to 360 μatm . In this context, we categorized the ECS into five different domains featured with different physics and biogeochemistry to better characterize the seasonality of the $p\text{CO}_2$ dynamics and to better constrain the CO_2 flux. The five domains are (I) the outer Changjiang estuary and Changjiang plume, (II) the Zhejiang–Fujian coast, (III) the northern ECS shelf, (IV) the middle ECS shelf, and (V) the southern ECS shelf. In spring and summer, $p\text{CO}_2$ off the Changjiang estuary was as low as $< 100 \mu\text{atm}$, while it was up to $> 400 \mu\text{atm}$ in fall. $p\text{CO}_2$ along the Zhejiang–Fujian coast was low in spring, summer and winter (300 to 350 μatm) but was relatively high in fall ($> 350 \mu\text{atm}$). In the northern ECS shelf, $p\text{CO}_2$ in summer and fall was $> 340 \mu\text{atm}$ in most areas, higher than in winter and spring. In the middle and southern ECS shelf, $p\text{CO}_2$ in summer ranged from 380 to 400 μatm , which was higher than in other seasons ($< 350 \mu\text{atm}$). The area-weighted CO_2 flux in the entire ECS shelf was $-10.0 \pm 2.0 \text{ mmol m}^{-2} \text{ d}^{-1}$ in winter, $-11.7 \pm 3.6 \text{ mmol m}^{-2} \text{ d}^{-1}$ in spring, $-3.5 \pm 4.6 \text{ mmol m}^{-2} \text{ d}^{-1}$ in summer and $-2.3 \pm 3.1 \text{ mmol m}^{-2} \text{ d}^{-1}$ in fall. It is

15 important to note that the standard deviations in these flux ranges mostly reflect the spatial variation of $p\text{CO}_2$, which differ from the spatial variance nor the bulk uncertainty. Nevertheless, on an annual basis, the average CO_2 influx into the entire ECS shelf was $-6.9 \pm 4.0 \text{ mmol m}^{-2} \text{ d}^{-1}$, about twice the global average in ocean margins.

20

Title Page

Abstract

Introduction

Conclusions

References

Tables

Figures



Back

Close

Full Screen / Esc

Printer-friendly Version

Interactive Discussion



1 Introduction

With the rapid growth of carbon flux measurements during the past decade, our estimation of the coastal ocean air–sea CO₂ fluxes have converged to a reasonably agreeable estimate of about 0.2 to 0.5 PgCyr⁻¹ at a global scale (Borges et al., 2005; Cai et al., 2006; Chen et al., 2013; Chen and Borges, 2009; Dai et al., 2013; Laruelle et al., 2010, 2014) and it is safe to state that the earlier estimate of up to 0.9 to 1.0 PgCyr⁻¹ was an overestimate. Having stated so, it remains, however, challenging to reliably assess the carbon fluxes in individual coastal systems that are often featured by the greatest variations in time and space both in terms of fluxes and their intrinsic controls. Understanding regional fluxes and controls is important both because it would affect global flux estimation, and in order to improve our modeling capability of the coastal ocean carbon cycle. A regional climate model that is particularly relevant to the societal sustainability would need an improved estimate of regional carbon fluxes to resolve its predictability of future changes. Finally, it has been recognized that anthropogenic activities have been increasingly embedded in many coastal oceans so that studying such human perturbation on carbon cycling remains challenging.

The East China Sea (ECS) is a shelf system featured with significant terrestrial input from a major world river from the west, the Changjiang (Yangtze River), as well as dynamic exchange at its eastern board with the Kuroshio, a major western ocean boundary current (Chen and Wang, 1999). Located in the temperate zone, the ECS is also characterized by a clear seasonal pattern with warm and productive summer, and cold and less productive winter (Gong et al., 2003; Han et al., 2013). Such a dynamic nature in both physical circulation and biogeochemistry make for large contrasts in different zones within the ECS and thus zonal based assessment is critical to reliably constrain the CO₂ flux in time and space in this important marginal sea.

Prior studies already reveal that the ECS is overall an annual net sink of the atmospheric CO₂ with remarkable seasonal variations (Chou et al., 2009, 2011; Kim et al., 2013; Peng et al., 1999; Shim et al., 2007; Tseng et al., 2011; Tsunogai et al.,

BGD

12, 5123–5167, 2015

Air–sea CO₂ fluxes in the East China Sea

X.-H. Guo et al.

Title Page

Abstract

Introduction

Conclusions

References

Tables

Figures



Back

Close

Full Screen / Esc

Printer-friendly Version

Interactive Discussion



Air–sea CO₂ fluxes in the East China Sea

X.-H. Guo et al.

[Title Page](#)[Abstract](#)[Introduction](#)[Conclusions](#)[References](#)[Tables](#)[Figures](#)[I ◀](#)[▶ I](#)[◀](#)[▶](#)[Back](#)[Close](#)[Full Screen / Esc](#)[Printer-friendly Version](#)[Interactive Discussion](#)

1999; Wang et al., 2000; Zhai and Dai, 2009). The ranges of present estimates are -3.3 to -6.5 $\text{mmol m}^{-2} \text{d}^{-1}$ in spring, -2.4 to -4.8 $\text{mmol m}^{-2} \text{d}^{-1}$ in summer, 0.4 to 2.9 $\text{mmol m}^{-2} \text{d}^{-1}$ in fall and -13.7 to -10.4 $\text{mmol m}^{-2} \text{d}^{-1}$ in winter. However, these estimates are either based on limited (only one or a few) field surveys (Chou et al., 2009, 2011; Peng et al., 1999; Shim et al., 2007; Tsunogai et al., 1999; Wang et al., 2000) or suffering from spatial limitation (Kim et al., 2013; Shim et al., 2007; Tsunogai et al., 1999; Zhai and Dai, 2009). Tseng et al. (2011) investigate the Changjiang Dilution Water induced CO₂ uptake in summer and obtain an empirical algorithm of surface water $p\text{CO}_2$ (partial pressure of CO₂) with the Changjiang river discharge and sea surface temperature (SST). Subsequently, they extrapolate the empirical algorithm to the entire ECS shelf and the whole year to obtain a significant CO₂ sink of 6.3 ± 1.1 $\text{mmol m}^{-2} \text{d}^{-1}$ (Tseng et al., 2011). With data from three field surveys conducted in spring, fall and winter added, Tseng et al. (2014) update the annual CO₂ flux in the ECS to be -4.9 ± 1.4 $\text{mmol m}^{-2} \text{d}^{-1}$ using the similar empirical algorithm method.

In this study, we investigated the air–sea CO₂ fluxes on the entire ECS shelf based on large scale observations during 24 mapping cruises from 2006 to 2011, resolving both spatial coverage and fully seasonal variations. This largest dataset, thus far, allowed for a better constraint of the carbon fluxes in this important ocean margin system. The estimate in an individual survey was based on the gridded average in five physically and biogeochemically distinct domains (Fig. 1), which were then averaged for each season and finally the annual average was calculated.

Domains I and II are essentially in the inner shelf shallower than 50 m, with Domain I being the core area of the outer Changjiang estuary and the near field Changjiang plume in warm seasons, while Domain II is off the Zhejiang–Fujian coast and featured by turbid coastal waters and the Changjiang plume in winter. Domains III, IV and V are all located in the mid- and outer shelf, influenced by the Kuroshio and thus characterized by lower nutrients and warm temperature. The difference is that Domain III is impacted by far field river plume in flood seasons but Domain IV is not (Bai et al., 2014). Domain V is characterized by upwelling off northern Taiwan. Based on the above con-

straint of seasonal and intra-seasonal variations in five spatially distinct (five physico-biogeochemical domains) and temporal (seasonal and intra-seasonal) scales, the distribution characteristics of the $p\text{CO}_2$ and the major controls in the ECS were better revealed. The final area-weighted average CO_2 flux in the entire ECS was estimated to be $-6.9(\pm 4.0) \text{ mmol m}^{-2} \text{ d}^{-1}$, which is \sim twice the global average of ocean margins, suggesting that the ECS is featured by a moderate to strong sink of atmospheric CO_2 . Our study also suggested that only part of the ECS shelf off the Changjiang estuary was river-dominated despite the large discharge of the Changjiang.

2 Study area

The ECS is one of the major marginal seas located in the western Pacific. The largest freshwater source to the ECS is the Changjiang, which delivers 940 km^3 freshwater annually with the highest discharge in summer (Dai and Trenberth, 2002). The circulation of the ECS is modulated by the East Asian monsoon. The northeast winds in winter last from September to April and the summer monsoon from the southwest is weaker and lasts from July to August. The Changjiang plume flows northeastward in summer but southwestward along the China coastline in winter (Lee and Chao, 2003). The northward flowing Kuroshio follows the isobaths beyond the shelf break at $\sim 200 \text{ m}$ (Lee and Chao, 2003; Liu and Gan, 2012). Near the shelf break, there are upwellings centered at the northeast of Taiwan Island and the southwest of Kyushu Island (Lee and Chao, 2003).

The SST in the ECS is low in winter and early spring but high in summer and early fall. The seasonal variation in SST is up to 10°C in the inner shelf and $\sim 5^\circ\text{C}$ in the outer shelf (Gong et al., 2003). In warm seasons, productivity in the ECS is as high as $> 1 \text{ g C m}^{-2} \text{ d}^{-1}$ (Gong et al., 2003). Changjiang freshwater and the upwelling of the Kuroshio subsurface water are believed to be the major sources of nutrients to the ECS shelf (Chen and Wang, 1999). Regulated by both productivity and temperature,

BGD

12, 5123–5167, 2015

Air–sea CO_2 fluxes in the East China Sea

X.-H. Guo et al.

Title Page

Abstract

Introduction

Conclusions

References

Tables

Figures

◀

▶

◀

▶

Back

Close

Full Screen / Esc

Printer-friendly Version

Interactive Discussion



$p\text{CO}_2$ shows strong seasonal variations, typically under-saturated in cold seasons and in productive areas in warm seasons (Chou et al., 2009, 2011; Tseng et al., 2011).

This study covers largely the entire ECS shelf (< 200 m). We categorized the ECS shelf into five distinct domains featured by different physico-biogeochemical characteristics based on the distributions of SST, chlorophyll *a* (chl *a*) concentration and turbidity (Fig. 1). The boundaries, surface areas and characteristics of the five domains are presented in Table 1 and Fig. 1.

Domain I (28.5–33.0° N, 122.0–126.0° E, $191 \times 10^3 \text{ km}^2$) is characterized by high chl *a* (He et al., 2013) and lowest $p\text{CO}_2$ in warm seasons. It covers most of the area within the 50 m isobaths. Domain II (25.0–28.5° N, 119.3–123.5° E, $41 \times 10^3 \text{ km}^2$) has a strong seasonal variation in $p\text{CO}_2$. Domain III (28.5–33.0° N, 126.0–128.0° E, $96 \times 10^3 \text{ km}^2$) is the northern ECS shelf generally dominated by temperature and impacted by the Changjiang plume in flood seasons. Domain IV (27.0–28.5° N, 123.5–128.0° E, $65 \times 10^3 \text{ km}^2$) is the middle ECS shelf characterized by low chl *a* all year round and high $p\text{CO}_2$ in warm seasons. Domain V (25.0–27.0° N, 120.0–125.4° E, $60 \times 10^3 \text{ km}^2$) is the southern ECS shelf where $p\text{CO}_2$ is dominated by temperature and might be under the influence of the northern Taiwan upwelling.

3 Material and methods

3.1 Measurements of $p\text{CO}_2$, SST, SSS and auxiliary data

24 cruises/legs were conducted from 2006 to 2011 in the ECS on board R/Vs *Dongfanghong II* and *Kexue III* or a fishing boat *Hubaoyu 2362*. Survey periods and areas are listed in Table 2. Sampling tracks are shown in Fig. 2. During the cruises, sea surface salinity (SSS), SST and $p\text{CO}_2$ were measured continuously. The methods of measurement and data processing followed those of Pierrot et al. (2009) and the SO-CAT (Surface Ocean CO_2 Atlas, <http://www.socat.info/news.html>) protocol, which are briefly summarized here.

BGD

12, 5123–5167, 2015

Air–sea CO_2 fluxes in the East China Sea

X.-H. Guo et al.

Title Page

Abstract

Introduction

Conclusions

References

Tables

Figures

◀

▶

◀

▶

Back

Close

Full Screen / Esc

Printer-friendly Version

Interactive Discussion



Air–sea CO₂ fluxes in the East China Sea

X.-H. Guo et al.

Title Page

Abstract

Introduction

Conclusions

References

Tables

Figures

I◀

▶I

◀

▶

Back

Close

Full Screen / Esc

Printer-friendly Version

Interactive Discussion



$p\text{CO}_2$ was continuously measured with a non-dispersive infrared spectrometer (Li-Cor[®] 7000) integrated in a GO-8050 underway system (General Oceanic Inc. USA) on board *Dongfanghong II* or with a home-made underway system on board *Kexue III* or *Hubaoyu 2362*. The GO-8050 underway system is described by Pierrot et al. (2009).

The home-made underway system is described by Zhai et al. (2007) and Zhai and Dai (2009), with which a Jiang et al. (2008) equilibrator was employed. Surface water was continuously pumped from 1.5 to 5 m depth and determined every 80 s. CO₂ concentration in the atmosphere was determined every ~ 1.5 h. The bow intake from which the air in the atmosphere was taken was installed ~ 10 m above the sea surface to avoid contamination from the ship. The barometric pressure was measured continuously aboard with a barometer attached to a level of ~ 10 m above the sea surface.

3.2 Data processing

Water $p\text{CO}_2$ at the temperature in the equilibrator ($p\text{CO}_2^{\text{Eq}}$) was calculated from the CO₂ concentration in the equilibrator ($x\text{CO}_2$) and the pressure in the equilibrator (P_{Eq}) after correction for the vapor pressure ($P_{\text{H}_2\text{O}}$) of water at 100 % relative humidity (Weiss and Price, 1980):

$$p\text{CO}_2^{\text{Eq}} = (P_{\text{Eq}} - P_{\text{H}_2\text{O}}) \times x\text{CO}_2 \quad (1)$$

$p\text{CO}_2$ in the air was calculated similarly using $x\text{CO}_2$ in the air and the barometric pressure using a formula similar to Eq. (1). $x\text{CO}_2$ in the atmosphere over the Taean Peninsula (36.7376° N, 126.1328° E, Republic of Korea, <http://www.esrl.noaa.gov/gmd/dv/site>) was adopted in the atmospheric $p\text{CO}_2$ calculation after comparison with the field measured values during the surveys.

Water $p\text{CO}_2^{\text{Eq}}$ obtained from Eq. (1) was corrected to $p\text{CO}_2$ at in situ temperature (in situ $p\text{CO}_2$, or $p\text{CO}_2$ hereafter) using the empirical formula of Takahashi et al. (1993), where t is the temperature in the equilibrator.

$$\text{In situ } p\text{CO}_2 = p\text{CO}_2^{\text{Eq}} \times \exp((\text{SST} - t) \times 0.0423) \quad (2)$$

Net CO₂ flux (F_{CO_2}) between the surface water and the atmosphere (or air–sea CO₂ flux) was calculated using the following formula:

$$F_{\text{CO}_2} = k \times s \times \Delta p\text{CO}_2 \quad (3)$$

where s is the solubility of CO₂ (Weiss, 1974); $\Delta p\text{CO}_2$ is the $p\text{CO}_2$ difference between the surface water and the atmosphere; and k is the CO₂ transfer velocity. k was parameterized using the empirical function of Sweeney et al. (2007) and nonlinear correction of gas transfer velocity with wind speed was adopted following Wanninkhof et al. (2002) and Jiang et al. (2008):

$$k(\text{S07}) = 0.27 \times C_2 \times U_{\text{mean}}^2 \times (\text{Sc}/660)^{-0.5} \quad (4)$$

$$C_2 = \left(\frac{1}{n} \sum_{j=1}^n U_j^2 \right) / U_{\text{mean}}^2 \quad (5)$$

where U_{mean} is the monthly mean wind speed at 10 m above the sea level (in m s^{-1}); and Sc is the Schmidt number at in situ temperature for surface seawater (Wanninkhof, 1992). C_2 is the nonlinear coefficient for the quadratic term of the gas transfer relationship; U_j is the high-frequency wind speed (in m s^{-1}); the subscript “mean” is to calculate the average; and n is the number of available wind speeds in the month. Wind speeds at a spatial resolution of $1^\circ \times 1^\circ$ and temporal resolution of 6 h were obtained from the National Centers for Environmental Prediction of the United States (NCEP, <http://oceandata.sci.gsfc.nasa.gov/Ancillary/Meteorological>) and the monthly average was adopted in the CO₂ flux calculations. As defined here, a positive flux indicates an evasion of CO₂ from the sea to the air.

$p\text{CO}_2$ normalized to a constant temperature of 21 °C, $Np\text{CO}_2$, was calculated following Takahashi et al. (2002):

$$Np\text{CO}_2 = p\text{CO}_2 \times \exp(0.0423 \times (21 - \text{SST})) \quad (6)$$

Air–sea CO₂ fluxes in the East China Sea

X.-H. Guo et al.

Title Page

Abstract

Introduction

Conclusions

References

Tables

Figures

◀

▶

◀

▶

Back

Close

Full Screen / Esc

Printer-friendly Version

Interactive Discussion



A temperature of 21 °C was used since it corresponded to the average SST during the cruises.

Our surveys covered the four seasons of the year, among which we defined March to May as spring, June to August as summer, September to November as fall and December to February as winter.

At the global scale, both the atmospheric $p\text{CO}_2$ and the surface seawater $p\text{CO}_2$ are increasing and the rate of increase differs in different regions (Takahashi et al., 2009). Tseng et al. (2014) report that the increasing rate of $p\text{CO}_2$ is 1.9 and 2.1 $\mu\text{atm yr}^{-1}$ for the atmosphere and the surface seawater, respectively, in the ECS. We thus corrected the atmospheric and surface water $p\text{CO}_2$ values to a reference year 2010 using the $p\text{CO}_2$ increasing rates.

4 Results

4.1 SST and SSS

Figure 3 reveals strong temporal and spatial variations in SST over the 12 months of the year. The seasonal variation in the average SST and SSS in the five domains is further shown in Fig. 4 and Tables 3 to 7. In winter and spring, SST increased offshore and from north to south with a range of ~ 8 to 25 °C, and the highest SST appeared in the southeastern part of the ECS. In summer and fall, SST was high and relatively spatially homogeneous compared to that in winter and spring with a range of ~ 18 to 30 °C. On a monthly time scale, the lowest SST appeared in January to March and the highest in July to September (Fig. 3). The magnitude of seasonal variation in SST decreased offshore, from 12 to 14 °C in Domains I and II to 6 to 8 °C in Domains IV and V. The lowest SST was observed in Domain I in January 2009, which was 8.1 ± 0.8 °C (Fig. 4). In July and August, there was a northeastern oriented filament with relatively low SST off eastern Taiwan (Fig. 3). The average SST measured underway during the

BGD

12, 5123–5167, 2015

Air–sea CO₂ fluxes in the East China Sea

X.-H. Guo et al.

Title Page

Abstract

Introduction

Conclusions

References

Tables

Figures

◀

▶

◀

▶

Back

Close

Full Screen / Esc

Printer-friendly Version

Interactive Discussion



surveys in the entire study area was $17.8 \pm 2.2^\circ\text{C}$ in winter, $19.7 \pm 2.9^\circ\text{C}$ in spring, $26.2 \pm 1.8^\circ\text{C}$ in summer and $23.2 \pm 1.2^\circ\text{C}$ in fall.

Spatially, salinity increased offshore and the highest salinity appeared in the area affected by the Kuroshio (not shown). At the whole shelf scale, the lowest salinity was observed in Domain I, where it was lower in March to August (29 to 32) and higher in September to February (30 to 34). The low SSS in spring and summer corresponded to the high freshwater discharge of the year from the Changjiang. SSS in June was relatively high compared to that in March, April, May, July and August (Fig. 4b), which might be attributed to the fact that there was only one June survey (June 2011) and this survey followed an exceptionally dry May. The discharge of the Changjiang in May of 2011 was $\sim 40\%$ lower than the monthly average of 2005 to 2011 (data at Datong gauge station, the *Hydrological Information Annual Report 2005 to 2011*, Ministry of Water Resources, China). On a seasonal scale, the average SSS in Domain I was lowest in spring (30.6 ± 4.6) and summer (30.9 ± 1.4) and highest in fall (33.4 ± 0.9). SSS in winter (31.5 ± 2.3) was higher than in spring-summer but lower than in fall. The seasonality of SSS in Domain II was different from that of Domain I (Table 3), and was lower in November to February (29.6 to 34.3) than in March to October (32.6 to 34.0, Fig. 4b). The lowest SSS was observed in winter (31.6 ± 0.9) and the highest in spring (33.4 ± 0.2) and summer (33.4 ± 0.3), whereas in fall (32.8 ± 1.1) it was between (Table 4). This seasonality might be attributed to the fact that the Changjiang plume and coastal current were southwestward in winter (Han et al., 2013; Lee and Chao, 2003). The seasonal variation of SSS in Domains I and II was up to 2.7 to 2.8.

Data in Domain III were rather limited, based on which, SSS in winter (34.4 ± 0.2) and fall (34.2 ± 0.1) was higher than that in summer (33.1 ± 0.6) (Table 5). The seasonality of SSS in Domains IV and V was similar, showing low SSS in July to September (33 to 34) but high in other months (> 34). Seasonal variation in SSS in these two domains was < 1 , which was much smaller than that in Domains I, II and III. The average salinity in the entire study area was 33.2 ± 2.5 in winter, 33.3 ± 4.7 in spring, 33.0 ± 1.6 in summer and 33.8 ± 1.3 in fall.

BGD

12, 5123–5167, 2015

Air–sea CO₂ fluxes in the East China Sea

X.-H. Guo et al.

Title Page

Abstract

Introduction

Conclusions

References

Tables

Figures

◀

▶

◀

▶

Back

Close

Full Screen / Esc

Printer-friendly Version

Interactive Discussion



4.2 Wind speeds and C_2

The temporal patterns of the wind speeds in the five domains were similar (Tables 3 to 7). The monthly average wind speeds ranged from 5.3 to 11.4 ms^{-1} and their standard deviations (SDs) were lower than 1 ms^{-1} . Generally, wind speed was high in fall and winter but low in spring and summer with great inter-annual variations. The highest wind speeds were recorded in Domains II, IV and V in November 2007, when the monthly average wind speeds reached 10.4 to 11.4 ms^{-1} . The lowest wind speeds were observed in August 2008, May 2009 and May 2011, when the monthly average wind speeds ranged from 5.6 to 6.5 ms^{-1} . Wind speeds in September, October and November 2006 were relatively low compared to other fall months and, in March 2009, were relatively high compared to other spring months.

C_2 ranged from 1.06 to 1.70 and the annual average C_2 in the five domains was 1.21 ± 0.04 , 1.20 ± 0.09 , 1.21 ± 0.06 , 1.19 ± 0.08 and 1.19 ± 0.13 , which was similar to or slightly lower than the global average of 1.27 (Wanninkhof et al., 2009).

4.3 CO_2 concentration in the air

Field observed CO_2 concentrations in the air over the ECS showed an increasing trend with a seasonal variation of ~ 10 to 20 ppm. Both the seasonal and inter annual patterns we measured during the surveys were similar to those observed at the Tae-ahn Peninsula (Korea–China Center for Atmospheric Research, Republic of Korea) with the highest values typically observed in February to April and the lowest values in July to September (Fig. 5). The difference in atmospheric CO_2 between our ship-board measurements over the ECS and that observed at the Tae-ahn Peninsula was not significant, ranging from 0.1 to 7.9 ppm (average ~ 3.5 ppm). However, the amplitude of the seasonal variation in air CO_2 concentration over the ECS was larger than that over the open North Pacific (Mauna Loa station), which was 5 to 10 ppm. Both the air CO_2 concentration over the ECS and the Tae-ahn Peninsula were higher than that at the Mauna

BGD

12, 5123–5167, 2015

Air–sea CO_2 fluxes in the East China Sea

X.-H. Guo et al.

Title Page

Abstract

Introduction

Conclusions

References

Tables

Figures

◀

▶

◀

▶

Back

Close

Full Screen / Esc

Printer-friendly Version

Interactive Discussion



Loa station, which might be due to the fact that the marine boundary atmosphere over marginal seas has more impacts from terrestrial sources.

4.4 Surface seawater $p\text{CO}_2$

$p\text{CO}_2$ values along the cruise tracks in this study are shown in Fig. 2. By averaging the $p\text{CO}_2$ values on these tracks to $1^\circ \times 1^\circ$ grids, we obtained the mean $p\text{CO}_2$ values in the five domains (Tables 3 to 7).

For the entire ECS shelf, $p\text{CO}_2$ was relatively homogeneous in winter but strong spatial variations occurred in other seasons (Fig. 2). In Domain I, $p\text{CO}_2$ was generally low ($< 360 \mu\text{atm}$) in winter, spring and summer except in the area off the Changjiang estuary mouth and in Hangzhou Bay and the northwestern corner which may be influenced by the southern Yellow Sea through the Yellow Sea Coastal Current (Su, 1998) that carried higher CO_2 water southward. However, in fall, $p\text{CO}_2$ was generally high ($> 380 \mu\text{atm}$) except in October 2006. In Domain II, both the seasonal evolution and the $p\text{CO}_2$ values were generally overall similar to those of Domain I, but $p\text{CO}_2$ in summer was higher than in Domain I based on the limited data (Fig. 2). In Domains I and II, the seasonal average $p\text{CO}_2$ values were 348 and 349 μatm in winter, 309 and 313 μatm in spring, 317 and 357 μatm in summer, and 393 and 388 μatm in fall (Tables 3 and 4). The seasonal pattern in Domains IV and V was different showing relatively low $p\text{CO}_2$ ($< 360 \mu\text{atm}$) in winter, spring and fall but high ($> 370 \mu\text{atm}$) in summer (Fig. 2). The seasonal average $p\text{CO}_2$ values in these two domains were 341 and 344 μatm in winter, 318 and 345 μatm in spring, 380 and 381 μatm in summer and 336 and 348 μatm in fall (Tables 6 and 7). Temporal coverage was sparse in Domain III. Based on the limited data, the seasonality of $p\text{CO}_2$ in Domain III was similar to those of Domains IV and V (Table 5). The seasonal variation was largest in Domains I, II and III (~ 80 to 90 μatm) and smallest in Domain V (37 μatm).

In addition to the strong seasonal variation, intra-seasonal variation was also remarkable. In Domain I, the intra-seasonal variation in $p\text{CO}_2$ was ~ 30 to 73 μatm during the winter, spring and summer cruises, but relatively smaller in fall ($< 10 \mu\text{atm}$ excluding

BGD

12, 5123–5167, 2015

Air–sea CO_2 fluxes in the East China Sea

X.-H. Guo et al.

Title Page

Abstract

Introduction

Conclusions

References

Tables

Figures

◀

▶

◀

▶

Back

Close

Full Screen / Esc

Printer-friendly Version

Interactive Discussion



the October 2006 and December 2010 surveys, Table 3). In Domain II, it was much smaller in winter ($< 10 \mu\text{atm}$) than in other seasons (30 to $80 \mu\text{atm}$, Table 4). In Domains IV and V, it was $\sim 10 \mu\text{atm}$ in winter, but relatively higher variability occurred in spring and summer (14 to $55 \mu\text{atm}$, Tables 6 and 7).

Based on the seasonal average as shown in Fig. 6, the overall characteristics were remarkable. In winter, the $p\text{CO}_2$ was relatively homogeneous and the average $p\text{CO}_2$ in each domain ranged from 340 to $349 \mu\text{atm}$. In spring, the gridded $p\text{CO}_2$ values were lower than those in winter except in the northwest corner and the area near the Changjiang estuary. The seasonal average $p\text{CO}_2$ values in the domains were generally lower than in winter (309 ± 60 , 313 ± 24 , 290 ± 10 , 318 ± 17 and $345 \pm 12 \mu\text{atm}$ in the five domains respectively) since the high $p\text{CO}_2$ values were located in very limited grids. In summer, $p\text{CO}_2$ was lower in the inner shelf and higher in the outer shelf with extremely high $p\text{CO}_2$ in the northwest corner and off the Changjiang estuary mouth and Hangzhou Bay. The seasonal average $p\text{CO}_2$ was 317 ± 72 , 357 ± 22 , 341 ± 18 , 380 ± 9.0 and $381 \pm 16 \mu\text{atm}$ in the five domains. In fall, the average $p\text{CO}_2$ was $393 \pm 40 \mu\text{atm}$ in Domain I, which was significantly higher than in the offshore domains (336 to $367 \mu\text{atm}$).

It is worth noting that the two cruises conducted in October 2006 and December 2010 appeared to be atypical. The results in these two cruises were significantly different from other surveys in the respective seasons. In the October 2006 cruise, the $p\text{CO}_2$ went down to $364 \mu\text{atm}$ in Domain I and $308 \mu\text{atm}$ in Domain II, which was 29 and $80 \mu\text{atm}$ lower than the averages of other fall cruises in the two domains. In the December 2010 cruise, $p\text{CO}_2$ in Domain I was up to $384 \mu\text{atm}$, which was $36 \mu\text{atm}$ higher than the average $p\text{CO}_2$ of the other winter cruises (Fig. 6). We will further discuss these cruises in Sect. 5.

The distribution of the SD of $p\text{CO}_2$ showed strong spatial and seasonal variations with a large range of 1 to $185 \mu\text{atm}$ (Fig. 6). In Domain I, the SD was low in winter and high in spring and summer. The highest SD occurred in summer in the coastal area off the Changjiang estuary mouth and in Hangzhou Bay with the highest value of

[Title Page](#)[Abstract](#)[Introduction](#)[Conclusions](#)[References](#)[Tables](#)[Figures](#)[Back](#)[Close](#)[Full Screen / Esc](#)[Printer-friendly Version](#)[Interactive Discussion](#)

Air–sea CO₂ fluxes in the East China Sea

X.-H. Guo et al.

[Title Page](#)[Abstract](#)[Introduction](#)[Conclusions](#)[References](#)[Tables](#)[Figures](#)[I ◀](#)[▶ I](#)[◀](#)[▶](#)[Back](#)[Close](#)[Full Screen / Esc](#)[Printer-friendly Version](#)[Interactive Discussion](#)

80 to 185 μatm . The SD in Domain II ranged from 1 to 48 μatm with higher values in spring and summer. In Domain III, the range of SD was 1 to 19 μatm and showed no remarkable seasonal pattern. In Domains IV and V, the SD range was 1 to 29 μatm with relatively higher values in spring and fall but lower in winter and summer in Domain IV, and higher in spring and summer but lower in fall and winter in Domain V. Since $p\text{CO}_2$ distribution was generally homogeneous in winter except in December 2010, as expected, the SD in winter was relatively low and in > 85 % grids was < 10 μatm and the highest SD was 17 μatm . The SD in October 2006 in Domain I was higher than the other fall surveys and the SD in Domain I in December 2010 was higher than the other winter surveys.

It should be noted that the SD of $p\text{CO}_2$ represents the mixture of sources of uncertainty in the gridded $p\text{CO}_2$ data, the analytical error, the spatial variance, and the bias from undersampling. Wang et al. (2014) demonstrate that the analytical errors are almost the same on the ECS shelf and the latitudinal distribution of SD is similar to that of the spatial variance. Thus, higher SD usually reflects higher spatial variance and vice versa along latitudes. However, the SD was equivalent to neither the spatial variance nor the bulk uncertainty and the bias from undersampling may exert the greatest uncertainty on the gridded $p\text{CO}_2$ in grids with poor sampling coverage (Wang et al., 2014).

4.5 Air–sea CO₂ fluxes

Similar to the different seasonality of $p\text{CO}_2$ in the differing domains, the air–sea CO₂ fluxes also had strong seasonal variations in each domain and the seasonal pattern differed among the domains (Tables 3 to 7).

Domain I was a sink of atmospheric CO₂ during all the winter, spring and summer surveys with CO₂ fluxes ranging from -14.0 to -1.6 $\text{mmol m}^{-2} \text{d}^{-1}$. However, Domain I in fall was a weak source of 2.2 ± 6.8 $\text{mmol m}^{-2} \text{d}^{-1}$, with a flux range of 1.9 to

2.7 mmol m⁻² d⁻¹ (Table 3). The CO₂ fluxes we estimated were similar to those estimated by Zhai and Dai (2009) based on multiple observations.

Similar to Domain I, Domain II was also a strong sink in winter and spring with a CO₂ flux range of -15.7 to -7.5 mmol m⁻² d⁻¹. The seasonal average flux was -8.9 ± 1.4 mmol m⁻² d⁻¹ in winter and -10.7 ± 3.5 mmol m⁻² d⁻¹ in spring. The sink weakened in summer and the seasonal average CO₂ flux was -2.4 ± 3.3 mmol m⁻² d⁻¹. In fall, Domain II was a CO₂ source of 0.7 ± 4.1 mmol m⁻² d⁻¹ (Table 4).

Although considerable variability occurred, Domains III, IV and V were generally strong sinks in winter, spring and fall (-3.7 to -18.7 mmol m⁻² d⁻¹) but weak to moderate sources in summer (0 to 6.8 mmol m⁻² d⁻¹ except in June 2011 when it was a strong sink). On a seasonal time scale, CO₂ fluxes were -10.8 ± 1.4, -10.5 ± 1.3 and -10.0 ± 1.9 mmol m⁻² d⁻¹ in winter in Domains III, IV and V; -17.8 ± 3.1, -11.2 ± 2.2 and -6.8 ± 4.3 mmol m⁻² d⁻¹ in spring; -3.7 ± 5.1, -9.3 ± 0.5 and -8.4 ± 2.0 mmol m⁻² d⁻¹ in fall; and -4.6 ± 4.0, 1.0 ± 1.5 and 1.8 ± 2.8 mmol m⁻² d⁻¹ in summer (Tables 5–7).

The annual mean CO₂ fluxes were -6.2 ± 9.1 mmol m⁻² d⁻¹ in Domain I, -5.3 ± 3.7 mmol m⁻² d⁻¹ in Domain II, -9.2 ± 4.2 mmol m⁻² d⁻¹ in Domain III, -7.5 ± 1.7 mmol m⁻² d⁻¹ in Domain IV and -5.9 ± 3.4 mmol m⁻² d⁻¹ in Domain V (Fig. 7). The area-weighted annual mean CO₂ flux was -6.9(±4.0) mmol m⁻² d⁻¹ (Fig. 7), which was more than twice the global average of ocean margins (Chen et al., 2013; Dai et al., 2013). Based on these CO₂ fluxes, the five domains absorbed 4.9(±4.4), 0.9(±0.4), 3.8(±1.0), 2.1(±0.3) and 1.5(±0.5) × 10¹² g C yr⁻¹, and the ECS shelf 13.2(±4.6) × 10¹² g C yr⁻¹ of atmospheric CO₂.

BGD

12, 5123–5167, 2015

Air–sea CO₂ fluxes in the East China Sea

X.-H. Guo et al.

Title Page

Abstract

Introduction

Conclusions

References

Tables

Figures

◀

▶

◀

▶

Back

Close

Full Screen / Esc

Printer-friendly Version

Interactive Discussion



5 Discussion

5.1 Major controls of surface water $p\text{CO}_2$

The CO_2 sink is dominated by the high biological productivity in summer (Chou et al., 2009), which appears to have close correlation with the Changjiang riverine discharge (Tseng et al., 2011, 2014). However, cooling is attributed to be the major driver of the CO_2 sink in winter (Tsunogai et al., 1999). In the northern ECS and the area off the Changjiang estuary, vertical mixing of the CO_2 -rich subsurface/bottom water is attributed to the CO_2 source in fall (Kim et al., 2013; Zhai and Dai, 2009). Shim et al. (2007) suggest that the $p\text{CO}_2$ in the northeastern ECS is dominated by temperature but the main controlling factor in the northwestern ECS is more seasonally complex. Based on the data collected from one cruise in summer, fall and winter, Chou et al. (2013) suggest that $p\text{CO}_2$ is dominated by biological production on the inner shelf and by temperature on the outer shelf.

Because of the significant zonal difference in seasonality shown in both $p\text{CO}_2$ and CO_2 fluxes, we discuss the major controls of $p\text{CO}_2$ in the five domains categorized. This discussion is primarily based on the relationships of the in situ and normalized $p\text{CO}_2$ ($Np\text{CO}_2$, normalized to 21°C in this study) with the other parameters in each domain. Since the Changjiang plume and coastal regions are strongly influenced by biological activities and/or the terrestrial high- $p\text{CO}_2$ waters (Tseng et al., 2014; Zhai and Dai, 2009), we used the data collected from the offshore area (Domains IV and V) to obtain the “background” $Np\text{CO}_2$. In these two domains, $Np\text{CO}_2$ ranged from 250 to $400\ \mu\text{atm}$, and so we used $250 \times \exp((\text{SST} - 21) \times 0.0423)$ and $400 \times \exp((\text{SST} - 21) \times 0.0423)\ \mu\text{atm}$ as the lower and upper limits of thermodynamically dominated $p\text{CO}_2$ on the entire ECS shelf.

In Domains I and II, $p\text{CO}_2$ showed no trend with SST and many $p\text{CO}_2$ data were beyond the range of thermodynamically dominated $p\text{CO}_2$ (Fig. 8). In addition, $p\text{CO}_2$ in these two domains also showed no trend with salinity (Fig. 9). This suggested that other processes in addition to SST and estuarine mixing also played important roles

BGD

12, 5123–5167, 2015

Air–sea CO_2 fluxes in the East China Sea

X.-H. Guo et al.

Title Page

Abstract

Introduction

Conclusions

References

Tables

Figures

⏪

⏩

◀

▶

Back

Close

Full Screen / Esc

Printer-friendly Version

Interactive Discussion



in the $p\text{CO}_2$ variability, including aerobic respiration, biological productivity, terrestrial input and ventilation, amongst other factors.

The Changjiang river and estuarine water were characterized by high $p\text{CO}_2$ resulting mainly from aerobic respiration (Zhai et al., 2007). In Domain I, the area off the Changjiang estuary and the coastal area were influenced by the high- $p\text{CO}_2$ estuarine water (Fig. 2). On the other hand, in warm seasons, the plume water was stratified and biological productivity lowered the surface water $p\text{CO}_2$ as indicated by the high chl *a* concentration in spring and summer (Fig. 10). $Np\text{CO}_2$ generally decreased with the increase in chl *a* concentration. Although $p\text{CO}_2$ showed no relationship with SST or SSS, $Np\text{CO}_2$ showed a decreasing pattern with SST and the lowest $Np\text{CO}_2$ occurred in the warm seasons, which was consistent with the highest productivity (Figs. 8 and 10). In fall, vertical stratification collapsed and the CO_2 -enriched subsurface and bottom waters mixed into the surface and increased the surface water $p\text{CO}_2$. In winter and early fall, the cooling effect decreased $p\text{CO}_2$ and resulted in Domain I acting as a CO_2 sink in the cold seasons. If the $p\text{CO}_2$ in winter was taken as the reference, the calculated thermodynamically controlled $p\text{CO}_2$ in spring would be $379.3 \mu\text{atm}$. The observed $p\text{CO}_2$ in spring was $70.4 \mu\text{atm}$ lower than the thermodynamically mediated $p\text{CO}_2$. Similarly, if spring was taken as a reference, the thermodynamically mediated $p\text{CO}_2$ in summer would be $479.0 \mu\text{atm}$ and the observed $p\text{CO}_2$ was $161.8 \mu\text{atm}$ lower than this value. These differences might be the CO_2 drop mainly mediated by biological activities. Similarly, the observed $p\text{CO}_2$ was $100.5 \mu\text{atm}$ higher than the thermodynamically mediated $p\text{CO}_2$ ($293.0 \mu\text{atm}$) in fall, which might be due mainly to the mixing of the CO_2 -rich subsurface/bottom water in fall, when vertical mixing was enhanced. It should be noted that the CO_2 system is a buffer system and the $p\text{CO}_2$ response is much slower (Zhai et al., 2014). Therefore the above estimation is to explain the biological effect on $p\text{CO}_2$ qualitatively rather than to make an accurate calculation.

Controls of $p\text{CO}_2$ in Domain II were similar to but more complex than those in Domain I. Cooling and biological uptake were responsible for the strong sink in winter and spring. However, in summer biological uptake of CO_2 was limited since it was beyond

BGD

12, 5123–5167, 2015

Air–sea CO_2 fluxes in the East China Sea

X.-H. Guo et al.

Title Page

Abstract

Introduction

Conclusions

References

Tables

Figures

◀

▶

◀

▶

Back

Close

Full Screen / Esc

Printer-friendly Version

Interactive Discussion



the productive area (Fig. 10), so the CO_2 flux was controlled by both biological activities and heating effect. In fall, cooling was important in drawing down $p\text{CO}_2$ and the influence of vertical mixing was not significant since the hypoxia and thus the high- $p\text{CO}_2$ bottom water was limited to Domain I (Chen et al., 2007; Wang et al., 2012).

In Domains IV and V, $p\text{CO}_2$ in summer was higher than that in the other seasons (Fig. 2). The $p\text{CO}_2$ generally increased with SST but showed no trend with SSS (Figs 8 and 9). This suggests that temperature was an important factor influencing $p\text{CO}_2$. Neither $p\text{CO}_2$ nor $Np\text{CO}_2$ showed conspicuous trends with chl *a* concentration, and chl *a* concentration was relatively low ($< 2 \mu\text{g L}^{-1}$, Fig. 10). This suggests that, for a particular season, productivity was not the dominating process in the spatial distribution of $p\text{CO}_2$. Comparison among the seasons showed that the $Np\text{CO}_2$ was highest in winter and lowest in summer. This might be due to the weak mixing of the CO_2 -rich subsurface water in summer. Additionally, the lowest $Np\text{CO}_2$ values in summer might suggest that the potential biological uptake of CO_2 was strong in summer, although biological uptake was not a dominating factor. Although $Np\text{CO}_2$ was lowest in summer, in situ $p\text{CO}_2$ was highest, indicating that high temperature increased $p\text{CO}_2$ in the warm seasons. With similar calculations conducted in Domain I, the estimated $p\text{CO}_2$ drawdown would be 25 to 39 μatm in spring and summer and the $p\text{CO}_2$ increase in fall would range from 21 to 35 μatm due to enhanced vertical mixing. These values were much lower than the dynamic inshore areas (Domains I and II) and might be negligible since the above estimations were very rough and the re-equilibrium of CO_2 takes a longer time than any particular season (Zhai et al., 2014). The major controls of $p\text{CO}_2$ in Domain III were between those of Domains I/II and IV/V.

In summary, the ECS shelf is heterogeneous in both CO_2 fluxes and their controls. The $p\text{CO}_2$ of the inner shelf waters (Domains I and II) was mainly dominated by the biological uptake of CO_2 in spring/summer and cooling in winter, which induced the moderate to strong sink in the three seasons, while in fall mixing with CO_2 -rich bottom/subsurface water was attributed to the CO_2 release. However, the offshore areas (Domains IV and V) were dominated mainly by temperature.

Air–sea CO_2 fluxes in the East China Sea

X.-H. Guo et al.

[Title Page](#)[Abstract](#)[Introduction](#)[Conclusions](#)[References](#)[Tables](#)[Figures](#)[I ◀](#)[▶ I](#)[◀](#)[▶](#)[Back](#)[Close](#)[Full Screen / Esc](#)[Printer-friendly Version](#)[Interactive Discussion](#)

Based on the data collected mainly in the inner and middle ECS shelves and limited field surveys in cold seasons, Tseng et al. (2014) suggest that the Changjiang discharge is the primary factor that governs the CO₂ sink for the entire ECS. The dataset covering complete seasonal and spatial coverage presented in this study suggested that zonal assessment is important to obtain a comprehensive picture of CO₂ flux and its control in the dynamic marginal seas. Extrapolation from the data collected in the river-dominated area to the entire ECS shelf could be misleading.

5.2 Intra-seasonal variation in CO₂ fluxes

With the five domains categorized, we have seen overall well defined seasonality in both $p\text{CO}_2$ and CO₂ fluxes in the individual domains, and significant intra-seasonal changes occurred, which could affect the overall carbon budgeting on a longer seasonal and/or annual time scale.

The intra-seasonal variation in the CO₂ fluxes was generally low in winter (within 2.1 fold variability), but it was very high in summer (4 to 6 fold) and spring (2 to 3 fold). Spatially, the largest intra-seasonal variability was in Domain I. The intra-seasonal variation in the calculated CO₂ flux in this study was attributed to the intra-seasonal variability in $\Delta p\text{CO}_2$, wind speeds, and C_2 . In the five domains, the highest value of C_2 was 1.1 to 1.4 fold of the lowest value within each season, which did not induce remarkable intra-seasonal variability in the calculated CO₂ flux. However, intra-seasonal variability in wind speed and $\Delta p\text{CO}_2$ might have induced large variability in the calculated CO₂ fluxes. The highest wind speed was 1.1 to 1.2 fold the lowest value in winter and 1.2 to 1.6 fold those in spring, summer and fall in each domain. This might have caused 1.2 to 1.4 fold variation in winter and 1.4 to 2.6 fold variation in other seasons in the calculated CO₂ fluxes. The intra-seasonal variability in wind speed showed no spatial pattern. The intra-seasonal variation in $\Delta p\text{CO}_2$ was generally high in summer and spring but low in winter and fall. The largest intra-seasonal variation was observed in Domain I in summer and spring. In summer, the lowest $\Delta p\text{CO}_2$ was $-85 \mu\text{atm}$ in June 2006, which was

BGD

12, 5123–5167, 2015

Air–sea CO₂ fluxes in the East China Sea

X.-H. Guo et al.

Title Page

Abstract

Introduction

Conclusions

References

Tables

Figures

◀

▶

◀

▶

Back

Close

Full Screen / Esc

Printer-friendly Version

Interactive Discussion



6.9 fold that in July 2009 ($-12 \mu\text{atm}$). The intra-seasonal variation in $\Delta p\text{CO}_2$ in spring was smaller than in summer but still very large (3.5 fold).

Additionally, atypical surveys increased the intra-seasonal variations. One example was the October 2006 cruise. Under typical fall conditions, Domain I is a source of atmospheric CO_2 when stratification starts to weaken and strong vertical mixing starts leading to the release of subsurface CO_2 (Zhai and Dai, 2009). In October 2006, however, average $p\text{CO}_2$ was down to $364 \mu\text{atm}$ in Domain I, which was $29 \mu\text{atm}$ lower than the seasonal average based on the data collected during all the other surveys in fall ($394 \mu\text{atm}$) (Table 3). The low $p\text{CO}_2$ in October 2006 might be induced by a local bloom which was reflected by the high oxygen saturation degree in the surface water. Dissolved oxygen increased to 120 to 130 % in a local area off Hangzhou Bay and the Changjiang estuary, which was a significant increase from September 2006 when the oxygen saturation degree ranged from 90 to 110 % (Fig. S1 in the Supplement). This local bloom caused Domain I to act as a CO_2 sink of $1.9 \text{ mmol m}^{-2} \text{ d}^{-1}$ as compared to a CO_2 source of $2.2 \text{ mmol m}^{-2} \text{ d}^{-1}$ based on the data collected from all the other fall surveys (Table 3). If this survey was included in the seasonal average CO_2 flux estimation, the seasonal average CO_2 flux in fall would be 1.2 ± 6.4 in Domain I and $-2.0 \pm 4.3 \text{ mmol m}^{-2} \text{ d}^{-1}$ in Domain II. This CO_2 source in Domain I was only 54 % of the previously estimated CO_2 flux in fall and Domain II would shift from a CO_2 source ($0.7 \text{ mmol m}^{-2} \text{ d}^{-1}$) to a CO_2 sink. However, including the October 2006 survey into the fall cruises had little influence on the annual CO_2 flux estimate (-7.0 vs. $-6.9 \text{ mmol m}^{-2} \text{ d}^{-1}$), which was attributed to the multiple observations in fall. Nevertheless, if the October 2006 were taken to represent fall, the annual CO_2 flux in the entire ECS would be $-7.9 \pm 3.9 \text{ mmol m}^{-2} \text{ d}^{-1}$, the CO_2 sink of which was 14 % stronger.

In the temperate seas, blooms occur in both spring and fall, which are mainly controlled by light availability and nutrient supply (Lalli and Parsons, 1993; Martinez et al., 2011). In the ECS, there is no report on fall blooms in the near shore area. The occurrence of a fall bloom and its influence on the CO_2 flux needs further study.

BGD

12, 5123–5167, 2015

Air–sea CO_2 fluxes in the East China Sea

X.-H. Guo et al.

Title Page

Abstract

Introduction

Conclusions

References

Tables

Figures

◀

▶

◀

▶

Back

Close

Full Screen / Esc

Printer-friendly Version

Interactive Discussion



Air–sea CO₂ fluxes in the East China Sea

X.-H. Guo et al.

[Title Page](#)[Abstract](#)[Introduction](#)[Conclusions](#)[References](#)[Tables](#)[Figures](#)[I◀](#)[▶I](#)[◀](#)[▶](#)[Back](#)[Close](#)[Full Screen / Esc](#)[Printer-friendly Version](#)[Interactive Discussion](#)

Another example is the early winter cruise (based on our seasonal category) in 2010 which was conducted on 1–11 December. The average SST was 5.5°C higher than the average SST during other winter surveys in Domain I. Also, the $p\text{CO}_2$ distribution pattern was similar to that in fall. As a result, Domain I was a weak sink of $-1.6\text{ mmol m}^{-2}\text{ d}^{-1}$ during this early December cruise, which was only 16% of the average CO_2 sink based on the data collected during the other winter cruises ($-9.8\text{ mmol m}^{-2}\text{ d}^{-1}$). We concluded that this early December 2010 survey was conducted during the transitional period between typical fall and winter, which would be difficult to be categorized into any season. If the December 2010 survey was grouped into the fall cruises, the seasonal average CO_2 flux in Domain I in fall would be $1.2 \pm 7.1\text{ mmol m}^{-2}\text{ d}^{-1}$ and the annual CO_2 flux in the entire ECS would be $-7.4 \pm 4.1\text{ mmol m}^{-2}\text{ d}^{-1}$. However, if the December 2010 survey was grouped into the winter cruises, the seasonal average CO_2 flux in Domain I in winter would be $-8.4 \pm 5.3\text{ mmol m}^{-2}\text{ d}^{-1}$ and the annual CO_2 flux in the entire ECS would be $-6.9 \pm 4.1\text{ mmol m}^{-2}\text{ d}^{-1}$.

This study reports what we believe to be a most comprehensive dataset of CO_2 fluxes based on field measurements with a full coverage of the ECS shelf at a temporal resolution of seasonal scale. Table 8 shows comparisons of the CO_2 fluxes estimated in this study with others in the ECS. For ease of comparison, we standardized the CO_2 flux estimation using the Sweeney et al. (2007) gas transfer velocity algorithms. For the results calculated using long-term (or monthly) average wind speeds, we multiplied C_2 (~ 1.2) to make them consistent with our estimation. The CO_2 fluxes calculated using the algorithm of Ho et al. (2006) were the same as those of Sweeney et al. (2007).

Comparison between our results and the CO_2 fluxes estimated based on multiple observations (such as those of Zhai and Dai, 2009) were similar in Domain I in all seasons. However, the CO_2 flux estimations based on limited surveys in spring, the season with strong intra-seasonal variability, such as those of Kim et al. (2013), Shim et al. (2007) and Peng et al. (1999), were often different from our results. However, the CO_2 flux based on a single survey in winter by Chou et al. (2011), Shim et al. (2007)

and Kim et al. (2013) were similar to our results, which is likely due to the relatively smaller inter-seasonal variability in winter. The CO₂ fluxes in spring and summer estimated by Tseng et al. (2011, 2014) are similar to our estimate based on field surveys. However, there is a large difference in the fall results. The good consistency of the Tseng et al. (2011, 2014) results with ours in spring and summer might be due to the fact that their empirical algorithm is mainly based on field data collected in warmer seasons.

We have demonstrated that field observations with full consideration of seasonal variability is necessary to constrain CO₂ fluxes with large heterogeneity in both time and space. We must point out, however, that it remains difficult to fully resolve the intra-seasonal changes in dynamic shelf seas. High-frequency observation and reducing the error from undersampling are mandatory to further improve estimates of CO₂ fluxes.

6 Concluding remarks

Surface water pCO₂ and air–sea CO₂ fluxes in the ECS shelf show strong temporal and spatial variations, despite which, the pCO₂ and associated fluxes are robustly well defined. The Changjiang plume is a moderate to strong CO₂ sink in spring, summer and winter, but it is a weak CO₂ source in fall. The middle and southern ECS shelves are a CO₂ source in summer but a strong CO₂ sink in other seasons. Major controls of pCO₂ differ in different domains. Domains I and II were mainly dominated by biological CO₂ uptake in spring and summer, ventilation in fall and cooling in winter, while Domains IV and V were dominated by temperature over the whole year. On an annual basis, the entire ECS shelf is a CO₂ sink of 6.9 (±4.0) mmol m⁻² d⁻¹ and it sequesters 13.2 Tg C from the atmosphere annually based on our observations from 2006 to 2011. This study suggested that zonal assessment of CO₂ fluxes and study of the major controls is necessary in the dynamic marginal seas.

BGD

12, 5123–5167, 2015

Air–sea CO₂ fluxes in the East China Sea

X.-H. Guo et al.

Title Page

Abstract

Introduction

Conclusions

References

Tables

Figures

⏪

⏩

◀

▶

Back

Close

Full Screen / Esc

Printer-friendly Version

Interactive Discussion



The Supplement related to this article is available online at
doi:10.5194/bgd-12-5123-2015-supplement.

Acknowledgements. This study was jointly supported by the National Basic Research Program of China through grant 2009CB421200 (the CHOICE-C project) and 2015CB954001 (CHOICE-C II), and Natural Science Foundation of China through grants 41076044 and 41121091, and the State Oceanic Administration of China through contract DOMEPP-MEA-01-10. Sampling cruises were partially supported by the National High-Tech Research and Development Program (“863” Program) of China (via the projects of Quality Control/in situ Standardization Experiment 2007 and 2008) and the National Basic Research Program of China (grant 2005CB422300). We are grateful to the crew and scientific staff of R/V *Dongfanghong II* for their help during these large-scale surveys. Yuancheng Su and Jinwen Liu are appreciated for the data collection during some of the cruises. Professor John Hodgkiss of The University of Hong Kong is thanked for polishing the English in this paper.

References

- Bai, Y., He, X., Pan, D., Chen, C.-T. A., Kang, Y., Chen, X., and Cai, W.-J.: Summertime Changjiang River plume variation during 1998–2010, *J. Geophys. Res.-Oceans*, 119, 6238–6257, 2014.
- Borges, A. V., Delille, B., and Frankignoulle, M.: Budgeting sinks and sources of CO₂ in the coastal ocean: diversity of ecosystems counts, *Geophys. Res. Lett.*, 32, L14601, doi:10.1029/2005GL023053, 2005.
- Cai, W.-J., Dai, M. H., and Wang, Y. C.: Air–sea exchange of carbon dioxide in ocean margins: a province-based synthesis, *Geophys. Res. Lett.*, 33, L12603, doi:10.1029/2006GL026219, 2006.
- Chen, C.-T. A., Huang, T.-H., Chen, Y.-C., Bai, Y., He, X., and Kang, Y.: Air–sea exchanges of CO₂ in the world’s coastal seas, *Biogeosciences*, 10, 6509–6544, doi:10.5194/bg-10-6509-2013, 2013.
- Chen, C. C., Gong, G. C., and Shiah, F. K.: Hypoxia in the East China Sea: one of the largest coastal low-oxygen areas in the world, *Marine Environ. Res.*, 64, 399–408, 2007.

BGD

12, 5123–5167, 2015

Air–sea CO₂ fluxes in the East China Sea

X.-H. Guo et al.

Title Page

Abstract

Introduction

Conclusions

References

Tables

Figures

◀

▶

◀

▶

Back

Close

Full Screen / Esc

Printer-friendly Version

Interactive Discussion



Air–sea CO₂ fluxes in the East China Sea

X.-H. Guo et al.

[Title Page](#)[Abstract](#)[Introduction](#)[Conclusions](#)[References](#)[Tables](#)[Figures](#)[I◀](#)[▶I](#)[◀](#)[▶](#)[Back](#)[Close](#)[Full Screen / Esc](#)[Printer-friendly Version](#)[Interactive Discussion](#)

Chen, C. T. A. and Borges, A. V.: Reconciling opposing views on carbon cycling in the coastal ocean: continental shelves as sinks and near-shore ecosystems as sources of atmospheric CO₂, *Deep-Sea Res. Pt. II*, 56, 578–590, 2009.

Chen, C. T. A. and Wang, S. L.: Carbon, alkalinity and nutrient budgets on the East China Sea continental shelf, *J. Geophys. Res.-Oceans*, 104, 20675–20686, 1999.

Chou, W.-C., Gong, G.-C., Sheu, D. D., Hung, C. C., and Tseng, T. F.: Surface distributions of carbon chemistry parameters in the East China Sea in summer 2007, *J. Geophys. Res.*, 114, C07026, doi:10.1029/2008JC005128, 2009.

Chou, W.-C., Gong, G.-C., Tseng, C. M., Sheu, D. D., Hung, C. C., Chang, L. P., and Wang, L. W.: The carbonate system in the East China Sea in winter, *Mar. Chem.*, 123, 44–55, 2011.

Chou, W.-C., Gong, G.-C., Cai, W.-J., and Tseng, C.-M.: Seasonality of CO₂ in coastal oceans altered by increasing anthropogenic nutrient delivery from large rivers: evidence from the Changjiang–East China Sea system, *Biogeosciences*, 10, 3889–3899, doi:10.5194/bg-10-3889-2013, 2013.

Dai, A. and Trenberth, K. E.: Estimates of freshwater discharge from continents: latitudinal and seasonal variations, *J. Hydrometeorol.*, 3, 660–687, 2002.

Dai, M. H., Cao, Z. M., Guo, X. H., Zhai, W. D., Liu, Z. Y., Yin, Z. Q., Xu, Y. P., Gan, J. P., Hu, J. Y., and Du, C. J.: Why are some marginal seas sources of atmospheric CO₂?, *Geophys. Res. Lett.*, 40, 2154–2158, 2013.

Gong, G.-C., Wen, Y. H., Wang, B. W., and Liu, G. J.: Seasonal variation of chlorophyll *a* concentration, primary production and environmental conditions in the subtropical East China Sea, *Deep-Sea Res. Pt. II*, 50, 1219–1236, 2003.

Han, A. Q., Dai, M. H., Gan, J. P., Kao, S.-J., Zhao, X. Z., Jan, S., Li, Q., Lin, H., Chen, C.-T. A., Wang, L., Hu, J. Y., Wang, L. F., and Gong, F.: Inter-shelf nutrient transport from the East China Sea as a major nutrient source supporting winter primary production on the northeast South China Sea shelf, *Biogeosciences*, 10, 8159–8170, doi:10.5194/bg-10-8159-2013, 2013.

He, X., Bai, Y., Pan, D., Chen, C.-T. A., Cheng, Q., Wang, D., and Gong, F.: Satellite views of the seasonal and interannual variability of phytoplankton blooms in the eastern China seas over the past 14 yr (1998–2011), *Biogeosciences*, 10, 4721–4739, doi:10.5194/bg-10-4721-2013, 2013.

Air–sea CO₂ fluxes in the East China Sea

X.-H. Guo et al.

Title Page

Abstract

Introduction

Conclusions

References

Tables

Figures

I ◀

▶ I

◀

▶

Back

Close

Full Screen / Esc

Printer-friendly Version

Interactive Discussion



- Ho, D. T., Law, C. S., Smith, M. J., Schlosser, P., Harvey, M., and Hill, P.: Measurements of air–sea gas exchange at high wind speeds in the Southern Ocean: implications for global parameterizations, *Geophys. Res. Lett.*, 33, L16611, doi:10.1029/2006GL026817, 2006.
- Jiang, L. Q., Cai, W. J., Wanninkhof, R., Wang, Y. C., and Luger, H.: Air–sea CO₂ fluxes on the US South Atlantic Bight: spatial and seasonal variability, *J. Geophys. Res.-Oceans*, 113, C07019, doi:10.1029/2007JC004366, 2008.
- Kim, D., Choi, S.-H., Shim, J.-H., Kim, K.-H., and Kim, C.-H.: Revisiting the seasonal variations of sea–air CO₂ fluxes in the northern East China Sea, *Terr. Atmos. Ocean. Sci.*, 24, 409–419, 2013.
- Lalli, C. M. and Parsons, T. R.: *Biological Oceanography: an Introduction*, Butterworth, Heine-
mann, Burlington, 1993.
- Laruelle, G. G., Durr, H. H., Slomp, C. P., and Borges, A. V.: Evaluation of sinks and sources of CO₂ in the global coastal ocean using a spatially-explicit typology of estuaries and continental shelves, *Geophys. Res. Lett.*, 37, L15607, doi:10.1029/2010GL043691, 2010.
- Laruelle, G. G., Ronny, L., Pfeil, B., and Regnier, P.: Regionalized global budget of the CO₂ exchange at the air–water interface in continental shelf seas, *Global Biogeochem. Cy.*, 28, 1199–1214, 2014.
- Lee, H. J. and Chao, S. Y.: A climatological description of circulation in and around the East China Sea, *Deep-Sea Res. Pt. II*, 50, 1065–1084, 2003.
- Liss, P. S. and Merlivat, L.: Air–sea gas exchange rates: introduction and synthesis, in: *The Role of Air–Sea Exchange in Geochemical Cycling*, edited by: Buat-Menard, P., Reidel, Hingham, MA, 113–129, 1986.
- Liu, Z. and Gan, J.: Variability of the Kuroshio in the East China Sea derived from satellite altimetry data, *Deep-Sea Res. Pt. I*, 59, 25–36, 2012.
- Martinez, E., Antoine, D., D’Ortenzio, F., and de Boyer Montegut, C.: Phytoplankton spring and fall blooms in the North Atlantic in the 1980s and 2000s, *J. Geophys. Res.*, 116, C11029, doi:10.1029/2010JC006836, 2011.
- Peng, T. H., Hung, J. J., Wanninkhof, R., and Millero, F. J.: Carbon budget in the East China Sea in spring, *Tellus B*, 51, 531–540, 1999.
- Pierrot, D., Neill, C., Sullivan, K., Castle, R., Wanninkhof, R., Luger, H., Johannessen, T., Olsen, A., Feely, R. A., and Cosca, C. E.: Recommendations for autonomous underway pCO₂ measuring systems and data-reduction routines, *Deep-Sea Res. Pt. II*, 56, 512–522, 2009.

Air–sea CO₂ fluxes in the East China Sea

X.-H. Guo et al.

Title Page

Abstract

Introduction

Conclusions

References

Tables

Figures

I ◀

▶ I

◀

▶

Back

Close

Full Screen / Esc

Printer-friendly Version

Interactive Discussion



Shim, J., Kim, D., Kang, Y. C., Lee, J. H., Jang, S. T., and Kim, C. H.: Seasonal variations in $p\text{CO}_2$ and its controlling factors in surface seawater of the northern East China Sea, *Cont. Shelf. Res.*, 27, 2623–2636, 2007.

Su, J.: Circulation dynamics of the China Seas north of ¹⁸N coastal segment, in: *The Sea*, Vol. 11, edited by: Robinson, A. R. and Brink, K. H., John Wiley & Sons, Inc., New York, 483–505, 1998.

Sweeney, C., Gloor, E., Jacobson, A. R., Key, R. M., McKinley, G., Sarmiento, J. L., and Wanninkhof, R.: Constraining global air–sea gas exchange for CO₂ with recent bomb C-14 measurements, *Global Biogeochem. Cy.*, 21, GB2015, doi:10.1029/2006GB002784, 2007.

Takahashi, T., Olafsson, J., Goddard, J. G., Chipman, D. W., and Sutherland, S. C.: Seasonal variation of CO₂ and nutrients in the high latitude surface oceans-A comparative study, *Global Biogeochem. Cy.*, 7, 843–878, 1993.

Takahashi, T., Sutherland, S. C., Sweeney, C., Poisson, A., Metzl, N., Tilbrook, B., Bates, N., Wanninkhof, R., Feely, R. A., Sabine, C., Olafsson, J., and Nojiri, Y.: Global sea–air CO₂ flux based on climatological surface ocean $p\text{CO}_2$, and seasonal biological and temperature effects, *Deep-Sea Res. Pt. II*, 49, 1601–1622, 2002.

Takahashi, T., Sutherland, S. C., Wanninkhof, R., Sweeney, C., Feely, R. A., Chipman, D. W., Hales, B., Friederich, G., Chavez, F., Sabine, C., Watson, A., Bakker, D. C. E., Schuster, U., Metzl, N., Yoshikawa-Inoue, H., Ishii, M., Midorikawa, T., Nojiri, Y., Kortzinger, A., Steinhoff, T., Hoppema, M., Olafsson, J., Arnarson, T. S., Tilbrook, B., Johannessen, T., Olsen, A., Bellerby, R., Wong, C. S., Delille, B., Bates, N. R., and de Baar, H. J. W.: Climatological mean and decadal change in surface ocean $p\text{CO}_2$, and net sea–air CO₂ flux over the global oceans, *Deep-Sea Res. Pt. II*, 56, 554–577, 2009.

Tans, P. P., Fung, I. Y., and Takahashi, T.: Observational constraints on the global atmospheric CO₂ budget, *Science*, 247, 1431–1438, 1990.

Tseng, C.-M., Liu, K. K., Gong, G. C., Shen, P. Y., and Cai, W. J.: CO₂ uptake in the East China Sea relying on Changjiang runoff is prone to change, *Geophys. Res. Lett.*, 38, L24609, doi:10.1029/2011GL049774, 2011.

Tseng, C.-M., Shen, P.-Y., and Liu, K.-K.: Synthesis of observed air–sea CO₂ exchange fluxes in the river-dominated East China Sea and improved estimates of annual and seasonal net mean fluxes, *Biogeosciences*, 11, 3855–3870, doi:10.5194/bg-11-3855-2014, 2014.

Tsunogai, S., Watanabe, S., and Sato, T.: Is there a “continental shelf pump” for the absorption of atmospheric CO₂?, *Tellus B*, 51, 701–712, 1999.

Air–sea CO₂ fluxes in the East China Sea

X.-H. Guo et al.

[Title Page](#)[Abstract](#)[Introduction](#)[Conclusions](#)[References](#)[Tables](#)[Figures](#)[I◀](#)[▶I](#)[◀](#)[▶](#)[Back](#)[Close](#)[Full Screen / Esc](#)[Printer-friendly Version](#)[Interactive Discussion](#)

Wang, B. D., Wei, Q. S., Chen, J. F., and Xie, L. P.: Annual cycle of hypoxia off the Changjiang (Yangtze River), *Estuar. Mar. Environ. Res.*, 77, 1–5, 2012.

Wang, G., Dai, M., Shen, S. S., Bai, Y., and Xu, Y.: Quantifying uncertainty sources in the gridded data of sea surface CO₂ partial pressure, *J. Geophys. Res.-Oceans*, 119, 5181–5189, 2014.

Wang, S. L., Chen, C. T. A., Hong, G. H., and Chung, C. S.: Carbon dioxide and related parameters in the East China Sea, *Cont. Shelf. Res.*, 20, 525–544, 2000.

Wanninkhof, R.: Relationship between wind speed and gas exchange over the ocean, *J. Geophys. Res.*, 97, 7373–7382, 1992.

Wanninkhof, R., Doney, S. C., Takahashi, T., and McGillis, W.: The effect of using time-averaged winds on regional air–sea CO₂ fluxes, in: *Gas Transfer at Water Surfaces*, edited by: Donelan, M. A., *Geophys. Monogr. Ser.*, Vol. 127, American Geophysical Union, Washington, D. C., doi:10.1029/GM127p0351, 351–357, 2002.

Wanninkhof, R., Asher, W. E., Ho, D. T., Sweeney, C., and McGillis, W. R.: Advances in quantifying air–sea gas exchange and environmental forcing, *Annu. Rev. Mar. Sci.*, 1, 213–244, 2009.

Weiss, R. F.: Carbon dioxide in water and seawater: the solubility of a non-ideal gas, *Mar. Chem.*, 2, 203–215, 1974.

Weiss, R. F. and Price, B. A.: Nitrous oxide solubility in water and seawater, *Mar. Chem.*, 8, 347–359, 1980.

Zhai, W., Chen, J., Jin, H., Li, H., Liu, J., He, X., and Bai, Y.: Spring carbonate chemistry dynamics of surface waters in the northern East China Sea: water mixing, biological uptake of CO₂, and chemical buffering capacity, *J. Geophys. Res.*, 119, 5638–5653, 2014.

Zhai, W. D. and Dai, M. H.: On the seasonal variation of air–sea CO₂ fluxes in the outer Changjiang (Yangtze River) Estuary, East China Sea. *Mar. Chem.*, 117, 2–10, 2009.

Zhai, W. D., Dai, M. H., and Guo, X. H.: Carbonate system and CO₂ degassing fluxes in the inner estuary of Changjiang (Yangtze) River, China. *Mar. Chem.*, 107, 342–356, 2007.

Air–sea CO₂ fluxes in the East China Sea

X.-H. Guo et al.

[Title Page](#)[Abstract](#)[Introduction](#)[Conclusions](#)[References](#)[Tables](#)[Figures](#)[I ◀](#)[▶ I](#)[◀](#)[▶](#)[Back](#)[Close](#)[Full Screen / Esc](#)[Printer-friendly Version](#)[Interactive Discussion](#)**Table 1.** Summary of the five physico-biogeochemical domains categorized in the East China Sea.

Domain	Location	Longitude (° E)	Latitude (° N)	Surface area (10 ⁴ km ²)	Description and characteristics
I	Outer Changjiang Estuary and Changjiang plume	122–126	28.5–33	19.1	Lower estuary beyond the turbidity maximum zone and inner shelf influenced by river plume.
II	Zhejiang-Fujian coast	119.33–123.5	25–28.5	4.1	Inner shelf dominated by turbid coastal waters with the influence of river plume primarily in winter.
III	Northern East China Sea	126–128	28.5–33	9.6	Mid- and outer shelf influenced by the Kuroshio. River plume signals visible in flood seasons.
IV	Middle East China Sea	122–128	27–28.5	6.5	Mid- and outer shelf influenced by the Kuroshio.
V	Southern East China Sea	120–125.42	25–27	6.0	Mid- and outer shelf influenced by the Kuroshio and characterized by upwelling northern Taiwan.

Air–sea CO₂ fluxes in the East China Sea

X.-H. Guo et al.

Title Page

Abstract

Introduction

Conclusions

References

Tables

Figures

◀

▶

◀

▶

Back

Close

Full Screen / Esc

Printer-friendly Version

Interactive Discussion

**Table 2.** Summary information of the 24 sampling surveys from 2006 to 2011.

Surveying time	Surveyed zones	Season	Sampling depth/RV	Sampler configuration	References/data source
1–3 Jan 2006	I	Winter	1.5 m (Fishing boat <i>Hubaoyu 2362</i>)	Modified from Zhai et al. (2007)	Zhai et al. (2007); Zhai and Dai (2009)
18–25 Sep 2006	I, II	Fall	3 m (<i>Kexue 3</i>)	Modified from Jiang et al. (2008)	This study ^a
14–17 Oct 2006	I, II, IV	Fall	3 m (<i>Kexue 3</i>)	Modified from Jiang et al. (2008)	This study ^a
20–24 Nov 2006	I, II	Fall	5 m (<i>Dongfanghong 2</i>)	Modified from Jiang et al. (2008)	This study ^a
2–6 Jul 2007	I, II, V	Summer	5 m (<i>Dongfanghong 2</i>)	Modified from Jiang et al. (2008)	This study ^a
1–10 Nov 2007	I, III	Fall	5 m (<i>Dongfanghong 2</i>)	GO8050	Zhai and Dai (2009)
20–30 Apr 2008	I, II	Spring	5 m (<i>Dongfanghong 2</i>)	GO8050	This study ^a
6–29 Aug 2008	I, II, IV, V	Summer	5 m (<i>Dongfanghong 2</i>)	GO8050	This study
23–31 Dec 2008	I, II, V	Winter	5 m (<i>Dongfanghong 2</i>)	GO8050	This study
10–14 Jan 2009	I, II	Winter	5 m (<i>Dongfanghong 2</i>)	GO8050	This study
15–31 Mar 2009	I, II, IV, V	Spring	5 m (<i>Dongfanghong 2</i>)	GO8050	This study
6–10 Apr 2009	I	Spring	1.5 m (<i>Hubaoyu 2362</i>)	Modified from Jiang et al. (2008)	This study
4–30 Apr 2009	I, II, III, IV, V	Spring	5 m (<i>Dongfanghong 2</i>)	GO8050	This study
1–13 May 2009	I, II, IV, V	Spring	5 m (<i>Dongfanghong 2</i>)	GO 8050	This study
1–3 Jul 2009	I, II, IV, V	Summer	5 m (<i>Dongfanghong 2</i>)	GO8050	Wang et al. (2014)
17–31 Aug 2009	I, II, III, IV, V	Summer	5 m (<i>Dongfanghong 2</i>)	GO8050	Wang et al. (2014)
4–31 Dec 2009	I, II, III, IV, V	Winter	5 m (<i>Dongfanghong 2</i>)	GO8050	This study
1–5 Jan 2010	II, IV, V	Winter	5 m (<i>Dongfanghong 2</i>)	GO8050	This study
1–6 Feb 2010	I, II	Winter	5 m (<i>Dongfanghong 2</i>)	GO8050	This study
26–30 Nov 2010	II, IV, V	Fall	5 m (<i>Dongfanghong 2</i>)	GO8050	This study
1–11 Dec 2010	I, III, IV	Winter	5 m (<i>Dongfanghong 2</i>)	GO8050	This study
13–15 Apr 2011	I, IV, V	Spring	5 m (<i>Dongfanghong 2</i>)	GO8050	This study
28–30 May 2011	II, III, IV, V	Spring	5 m (<i>Dongfanghong 2</i>)	GO8050	This study
1–8 Jun 2011	I, II, III, IV	Summer	5 m (<i>Dongfanghong 2</i>)	GO8050	This study

^a Partially published in Zhai and Dai (2009).

Table 3. Data summary of Domain I. Atm. $p\text{CO}_2$ is atmospheric $p\text{CO}_2$; SST is sea surface temperature; SSS is sea surface salinity; F_{CO_2} is the air–sea CO₂ flux; SD is the standard deviation. C_2 is the nonlinearity effect of the short-term variability of wind speeds over a month on the gas transfer velocity, assuming long-term winds followed a Raleigh (Weibull) distribution (Wanninkhof, 1992; Jiang et al., 2008). See text for details. October 2006 and December 2010 were excluded in the calculations of seasonal averages. $p\text{CO}_2$ data are corrected to the reference year 2010.

Season	Period	$p\text{CO}_2$ (μatm)		Atm. $p\text{CO}_2$ (μatm)		$\Delta p\text{CO}_2$ (μatm)		SST ($^{\circ}\text{C}$)		SSS		Wind speed (ms^{-1})		C_2	F_{CO_2} ($\text{mmolm}^{-2}\text{d}^{-1}$)		
		Mean	SD	Mean	SD	Mean	SD	Mean	SD	Mean	SD	Mean	SD		Mean	SD	
Winter	23–31 Dec 2008	356.4	7.2	392.2	0.3	−35.8	7.2	14.95	0.93	31.71	0.86	8.05	0.63	1.24	−7.91	2.16	
	4–31 Dec 2009	352.6	9.3	389.4	0.6	−36.8	9.3	15.66	1.05	32.71	0.96	8.24	0.91	1.19	−7.73	4.02	
	1–3 Jan 2006	360.7	17.5	395.4	1.6	−34.7	17.5	12.23	1.05	30.28	4.28	8.12	0.82	1.14	−6.46	6.90	
	1–14 Jan 2009	341.4	2.6	399.3	0.4	−58.0	2.6	8.07	0.79	29.98	0.73	8.42	0.89	1.20	−13.45	1.88	
	1–5 Jan 2010	–	–	–	–	–	–	–	–	–	–	7.95	0.85	1.22	–	–	
	1–6 Feb 2010	329.8	6.6	395.7	0.2	−65.9	6.6	11.27	0.73	32.65	0.45	7.86	0.72	1.21	−13.30	3.80	
	1–11 Dec 2010	384.2	19.7	390.3	0.5	−6.1	19.7	17.96	0.57	33.01	0.65	9.11	0.67	1.23	−1.59	7.50	
	Seasonal average	348.2	11.1	394.4	0.9	−46.2	11.1	12.44	1.03	31.47	2.28	8.11	0.89	1.20	−9.77	4.65	
	Spring	15–31 Mar 2009	359.4	13.4	391.9	0.4	−32.5	13.5	11.95	0.74	29.89	1.97	7.68	0.93	1.16	−5.75	6.15
		20–30 Apr 2008	315.6	53.0	396.5	0.7	−81.0	53.0	15.95	1.66	29.99	7.03	5.83	0.41	1.27	−9.87	5.96
4–30 Apr 2009		303.5	28.2	395.9	0.3	−92.3	28.2	15.12	0.75	31.21	0.79	5.94	0.42	1.26	−11.48	4.56	
6–10 Apr 2009		286.3	101.7	398.6	0.7	−112.3	101.7	13.53	1.07	29.83	6.85	5.94	0.42	1.26	−13.97	11.10	
12–15 Apr 2011		295.8	46.0	398.9	0.4	−103.1	46.0	12.38	0.69	32.42	0.62	6.25	0.31	1.25	−14.01	8.82	
1–20 May 2009		292.7	41.2	388.3	0.4	−95.6	41.2	17.84	0.61	30.28	1.45	5.43	0.26	1.20	−8.94	6.28	
26–31 May 2011		–	–	–	–	–	–	–	–	–	–	5.79	0.23	1.21	–	–	
Seasonal average		308.9	59.9	395.0	0.5	−86.1	59.9	14.46	1.08	30.60	4.55	6.12	0.52	1.23	−10.67	8.18	
Summer		1–12 Jul 2009	357.2	56.0	369.5	0.6	−12.3	56.0	23.34	0.64	30.47	1.18	6.40	0.52	1.18	−1.60	9.34
		2–6 Jul 2007	292.7	56.1	374.9	0.5	−82.1	56.1	24.53	0.69	30.69	1.50	5.57	0.77	1.27	−8.88	7.31
	6–29 Aug 2008	339.8	77.9	374.6	0.5	−34.8	77.9	28.00	0.61	31.02	1.16	5.41	0.50	1.21	−3.25	12.59	
	17–31 Aug 2009	293.8	64.5	362.8	0.6	−69.0	64.5	28.63	0.65	30.38	1.52	6.13	0.32	1.22	−8.42	9.72	
	1–19 Jun 2011	302.4	64.6	387.6	0.7	−85.2	64.6	19.67	0.68	32.08	0.76	5.85	0.49	1.27	−10.21	7.98	
	Seasonal average	317.2	71.9	373.9	0.6	−56.7	71.9	24.83	0.73	30.93	1.41	5.87	0.60	1.23	−6.47	10.69	
Fall	18–25 Sep 2006	387.8	50.0	374.9	0.7	12.9	50.0	25.27	0.34	33.34	1.08	7.01	0.56	1.19	2.71	5.81	
	14–18 Oct 2006	364.3	65.6	382.8	0.4	−18.5	65.6	25.20	0.37	33.47	1.67	6.12	0.61	1.13	−1.87	5.53	
	20–24 Nov 2006	396.9	23.6	386.3	0.3	10.6	23.6	20.88	0.43	32.93	0.46	7.74	0.69	1.17	1.88	3.73	
	1–10 Nov 2007	395.7	14.4	385.5	0.3	10.3	14.4	22.73	0.34	33.95	0.17	8.14	1.06	1.13	1.88	6.77	
	26–30 Nov 2010	–	–	–	–	–	–	–	–	–	–	6.73	0.74	1.22	–	–	
	Seasonal average	393.5	40.4	382.2	0.6	11.3	40.4	22.96	0.46	33.41	0.84	7.41	0.91	1.17	2.16	6.84	
Annual average	341.9	59.2	386.4	0.8	−44.4	59.2	18.67	1.00	31.60	3.08	6.88	0.86	1.21	−6.19	9.12		

Title Page

Abstract

Introduction

Conclusions

References

Tables

Figures

◀

▶

◀

▶

Back

Close

Full Screen / Esc

Printer-friendly Version

Interactive Discussion



Table 4. Data summary of Domain II. Atm. $p\text{CO}_2$ is atmospheric $p\text{CO}_2$; SST is sea surface temperature; SSS is sea surface salinity; F_{CO_2} is the air–sea CO₂ flux; SD is its standard deviation. C_2 is the nonlinearity effect of the short-term variability of wind speeds over a month on the gas transfer velocity, assuming long-term winds followed a Raleigh (Weibull) distribution (Wanninkhof, 1992; Jiang et al., 2008). See text for details. October 2006 and December 2010 were excluded in the calculations of seasonal averages. $p\text{CO}_2$ data are corrected to the reference year 2010.

Season	Period	$p\text{CO}_2$ (μatm)		Atm. $p\text{CO}_2$ (μatm)		$\Delta p\text{CO}_2$ (μatm)		SST ($^{\circ}\text{C}$)		SSS		Wind speed (m s^{-1})		C_2	F_{CO_2} ($\text{mmol m}^{-2} \text{d}^{-1}$)		
		Mean	SD	Mean	SD	Mean	SD	Mean	SD	Mean	SD	Mean	SD	Mean	Mean	SD	
Winter	23–31 Dec 2008	350.3	8.0	389.0	0.9	−38.6	8.1	16.15	1.70	30.59	1.38	8.56	0.99	1.18	−8.74	1.41	
	4–31 Dec 2009	343.8	7.7	389.8	0.6	−46.1	7.7	19.37	0.66	34.26	0.26	8.02	0.74	1.17	−8.74	0.28	
	1–3 Jan 2006	–	–	–	–	–	–	–	–	–	–	–	–	–	–	–	
	1–14 Jan 2009	347.7	4.5	395.0	0.3	−47.3	4.5	12.56	0.52	29.64	0.47	9.01	1.02	1.12	−10.89	0.90	
	1–5 Jan 2010	353.0	9.3	391.4	1.5	−38.4	9.4	16.64	1.61	32.38	0.91	7.90	0.76	1.22	−7.82	1.85	
	1–6 Feb 2010	352.4	7.2	392.5	0.5	−40.1	7.2	12.73	0.65	31.19	0.49	7.98	0.59	1.20	−8.25	1.35	
	1–11 Dec 2010	–	–	–	–	–	–	–	–	–	–	–	–	–	–	–	
	Seasonal average	349.4	8.4	391.5	1.0	−42.1	8.4	15.49	1.29	31.61	0.90	8.36	0.92	1.18	−8.89	1.42	
	Spring	15–31 Mar 2009	308.5	13.4	389.6	0.5	−81.1	13.4	18.52	0.76	34.01	0.23	8.30	0.69	1.14	−15.72	2.61
		20–30 Apr 2008	331.2	22.5	392.0	1.1	−60.9	22.6	21.76	1.73	33.83	0.82	6.38	0.53	1.19	−7.54	3.31
4–30 Apr 2009		312.4	11.7	392.1	0.3	−79.7	11.7	20.14	0.15	34.01	0.06	7.00	0.97	1.17	−11.50	1.69	
6–10 Apr 2009		–	–	–	–	–	–	–	–	–	–	7.00	0.97	1.17	–	–	
12–15 Apr 2011		–	–	–	–	–	–	–	–	–	–	6.57	0.52	1.24	–	–	
1–20 May 2009		290.6	35.8	386.7	0.7	−96.1	35.8	21.47	1.13	32.63	1.47	5.67	0.56	1.18	−9.36	3.97	
26–31 May 2011		323.1	11.9	394.8	0.9	−71.7	11.9	22.23	0.21	32.63	0.56	6.26	0.42	1.23	−9.14	3.42	
Seasonal average		313.2	23.7	391.1	0.8	−77.9	23.7	20.82	1.11	33.42	0.89	6.74	0.75	1.19	−10.65	3.47	
Summer	1–12 Jul 2009	361.4	16.9	367.1	0.4	−5.7	16.9	26.59	0.31	33.51	0.22	6.33	0.51	1.19	−0.69	2.04	
	2–6 Jul 2007	346.9	11.8	373.5	0.4	−26.6	11.8	26.48	0.75	33.81	0.31	6.86	0.59	1.21	−3.89	1.64	
	6–29 Aug 2008	397.3	2.9	374.7	0.3	22.6	2.9	28.76	0.46	33.40	0.28	5.56	0.40	1.23	2.26	0.28	
	17–31 Aug 2009	363.3	38.0	362.8	0.3	0.5	38.0	28.82	0.33	33.06	0.47	6.19	0.27	1.52	0.09	5.95	
	1–19 Jun 2011	318.6	0.3	387.7	1.6	−69.1	1.6	21.19	0.04	33.40	0.02	6.78	0.43	1.18	−9.51	0.04	
	Seasonal average	357.5	21.7	373.2	0.9	−15.7	21.7	26.37	0.49	33.44	0.33	6.34	0.51	1.27	−2.35	3.25	
Fall	18–25 Sep 2006	407.5	14.2	374.8	0.6	32.8	14.2	26.14	0.19	33.04	0.31	7.28	0.77	1.19	5.24	3.02	
	14–18 Oct 2006	308.4	25.3	381.6	0.2	−73.3	25.3	25.69	0.12	33.37	0.43	7.17	1.07	1.12	−10.05	4.69	
	20–24 Nov 2006	377.7	8.1	377.7	8.1	0.0	11.4	23.07	0.30	33.23	0.34	6.97	0.75	1.18	−0.99	1.15	
	1–10 Nov 2007	–	–	–	–	–	–	–	–	–	–	10.81	1.40	1.07	–	–	
	26–30 Nov 2010	378.5	16.4	388.5	0.6	−10.1	16.5	19.47	1.00	32.00	1.40	9.01	1.29	1.10	−2.10	4.82	
	Seasonal average	387.9	16.4	380.3	5.7	7.6	17.4	22.89	0.75	32.76	1.05	8.52	1.26	1.13	0.71	4.10	
Annual average		352.0	21.4	384.0	3.4	−32.0	21.6	21.39	1.11	32.81	0.97	7.49	1.04	1.19	−5.29	3.72	

Table 5. Data summary of Domain III. Atm. $p\text{CO}_2$ is atmospheric $p\text{CO}_2$; SST is sea surface temperature; SSS is sea surface salinity; F_{CO_2} is the air–sea CO₂ flux; SD is its standard deviation. C_2 is the nonlinearity effect of the short-term variability of wind speeds over a month on the gas transfer velocity, assuming long-term winds followed a Raleigh (Weibull) distribution (Wanninkhof, 1992; Jiang et al., 2008). See text for details. October 2006 and December 2010 were excluded in the calculations of seasonal averages. $p\text{CO}_2$ data are corrected to the reference year 2010.

Season	Period	$p\text{CO}_2$ (μatm)		Atm. $p\text{CO}_2$ (μatm)		$\Delta p\text{CO}_2$ (μatm)		SST ($^{\circ}\text{C}$)		SSS		Wind speed (ms^{-1})		C_2	F_{CO_2} ($\text{mmol m}^{-2} \text{d}^{-1}$)	
		Mean	SD	Mean	SD	Mean	SD	Mean	SD	Mean	SD	Mean	SD	Mean	Mean	SD
Winter	23–31 Dec 2008	–	–	–	–	–	–	–	–	–	–	8.21	0.16	1.25	–	–
	4–31 Dec 2009	340.1	8.8	385.9	0.5	–45.7	8.8	19.57	0.75	34.38	0.15	8.86	0.30	1.18	–10.75	1.44
	1–3 Jan 2006	–	–	–	–	–	–	–	–	–	–	8.79	0.38	1.13	–	–
	1–14 Jan 2009	–	–	–	–	–	–	–	–	–	–	9.21	0.25	1.18	–	–
	1–5 Jan 2010	–	–	–	–	–	–	–	–	–	–	8.48	0.36	1.21	–	–
	1–6 Feb 2010	–	–	–	–	–	–	–	–	–	–	8.39	0.31	1.19	–	–
	1–11 Dec 2010	335.2	9.2	387.3	0.5	–52.2	9.2	22.26	0.48	34.42	0.04	9.79	0.51	1.20	–15.33	5.19
	Seasonal average	340.1	8.8	385.9	0.5	–45.7	8.8	19.57	0.75	34.38	0.15	8.66	0.30	1.19	–10.75	1.44
Spring	15–31 Mar 2009	–	–	–	–	–	–	–	–	–	–	8.81	0.36	1.13	–	–
	20–30 Apr 2008	–	–	–	–	–	–	–	–	–	–	6.68	0.38	1.21	–	–
	4–30 Apr 2009	289.5	10.4	396.2	0.8	–106.7	10.4	17.82	1.24	34.14	0.27	6.95	0.62	1.26	–17.76	3.14
	6–10 Apr 2009	–	–	–	–	–	–	–	–	–	–	6.95	0.62	1.26	–	–
	12–15 Apr 2011	–	–	–	–	–	–	–	–	–	–	6.93	0.27	1.24	–	–
	1–20 May 2009	–	–	–	–	–	–	–	–	–	–	6.17	0.41	1.20	–	–
	26–31 May 2011	–	–	–	–	–	–	–	–	–	–	5.61	0.25	1.25	–	–
	Seasonal average	289.5	10.4	396.2	0.8	–106.7	10.4	17.82	1.24	34.14	0.27	6.87	0.62	1.22	–17.76	3.14
Summer	1–12 Jul 2009	–	–	–	–	–	–	–	–	–	–	6.69	0.23	1.14	–	–
	2–6 Jul 2007	–	–	–	–	–	–	–	–	–	–	5.94	0.61	1.40	–	–
	6–29 Aug 2008	–	–	–	–	–	–	–	–	–	–	6.23	0.39	1.18	–	–
	17–31 Aug 2009	378.3	10.2	362.1	0.3	16.2	10.2	29.43	0.26	33.12	0.49	5.59	0.25	1.28	1.77	3.67
	1–19 Jun 2011	304.0	14.5	386.6	1.2	–82.6	14.5	19.25	0.84	33.34	0.35	6.10	0.65	1.28	–10.90	1.63
	Seasonal average	341.1	17.7	374.3	1.2	–33.2	17.8	24.34	0.88	33.23	0.60	6.11	0.52	1.26	–4.56	4.02
Fall	18–25 Sep 2006	–	–	–	–	–	–	–	–	–	–	7.08	0.88	1.20	–	–
	14–18 Oct 2006	–	–	–	–	–	–	–	–	–	–	7.03	0.59	1.14	–	–
	20–24 Nov 2006	–	–	–	–	–	–	–	–	–	–	7.82	0.52	1.17	–	–
	1–10 Nov 2007	367.3	8.6	384.9	0.3	–17.6	8.6	23.73	0.26	34.19	0.06	8.96	0.50	1.11	–3.70	5.06
	26–30 Nov 2010	–	–	–	–	–	–	–	–	–	–	7.40	0.20	1.17	–	–
	Seasonal average	367.3	8.6	384.9	0.3	–17.6	8.6	23.73	0.26	34.19	0.06	7.82	0.50	1.16	–3.70	5.06
Annual average	334.5	13.8	385.3	0.9	–50.8	13.8	21.37	0.99	33.98	0.39	7.36	0.57	1.21	–9.20	4.23	

Title Page	
Abstract	Introduction
Conclusions	References
Tables	Figures
◀	▶
◀	▶
Back	Close
Full Screen / Esc	
Printer-friendly Version	
Interactive Discussion	



Table 6. Data summary of Domain IV. Atm. $p\text{CO}_2$ is atmospheric $p\text{CO}_2$; SST is sea surface temperature; SSS is sea surface salinity; F_{CO_2} is the air–sea CO₂ flux; SD is its standard deviation. C_2 is the nonlinearity effect of the short-term variability of wind speeds over a month on the gas transfer velocity, assuming long-term winds followed a Raleigh (Weibull) distribution (Wanninkhof, 1992; Jiang et al., 2008). See text for details. October 2006 and December 2010 were excluded in the calculations of seasonal averages. $p\text{CO}_2$ data are corrected to the reference year 2010.

Season	Period	$p\text{CO}_2$ (μatm)		Atm. $p\text{CO}_2$ (μatm)		$\Delta p\text{CO}_2$ (μatm)		SST ($^{\circ}\text{C}$)		SSS		Wind speed (m s^{-1})		C_2	F_{CO_2} ($\text{mmol m}^{-2} \text{d}^{-1}$)	
		Mean	SD	Mean	SD	Mean	SD	Mean	SD	Mean	SD	Mean	SD	Mean	Mean	SD
Winter	23–31 Dec 2008	335.5	3.8	387.5	0.3	−52.0	3.8	20.60	0.59	34.04	0.32	8.85	0.34	1.16	−11.77	0.85
	4–31 Dec 2009	339.1	5.1	387.3	0.7	−48.2	5.1	20.13	0.84	34.55	0.08	8.60	0.19	1.19	−10.83	1.61
	1–3 Jan 2006	–	–	–	–	–	–	–	–	–	–	9.02	0.30	1.11	–	–
	1–14 Jan 2009	–	–	–	–	–	–	–	–	–	–	9.36	0.45	1.16	–	–
	1–5 Jan 2010	347.5	2.3	389.3	0.2	−41.8	2.3	19.06	0.27	34.46	0.12	8.42	0.30	1.19	−9.04	0.50
	1–6 Feb 2010	–	–	–	–	–	–	–	–	–	–	9.06	0.14	1.16	–	–
	1–11 Dec 2010	331.2	4.0	388.7	0.5	−57.5	4.1	22.63	0.46	34.46	0.04	8.96	0.17	1.22	−14.63	1.33
Seasonal average		340.7	4.8	388.0	0.6	−47.3	4.8	19.93	0.75	34.35	0.25	8.89	0.33	1.17	−10.55	1.34
Spring	15–31 Mar 2009	305.8	13.5	387.6	0.7	−81.8	13.5	21.34	0.98	34.36	0.10	9.15	0.20	1.13	−18.69	3.09
	20–30 Apr 2008	–	–	–	–	–	–	–	–	–	–	7.07	0.21	1.17	–	–
	4–30 Apr 2009	326.3	16.0	391.6	0.8	−65.4	16.1	21.52	1.34	33.99	0.52	7.57	0.37	1.15	−10.62	0.65
	6–10 Apr 2009	–	–	–	–	–	–	–	–	–	–	7.57	0.37	1.15	–	–
	12–15 Apr 2011	317.3	17.5	396.3	1.0	−79.0	17.6	18.37	1.45	34.43	0.34	6.88	0.08	1.18	−11.25	0.92
	1–20 May 2009	300.1	20.1	388.6	0.8	−88.6	20.1	21.03	1.31	33.81	0.44	5.98	0.22	1.16	−9.17	2.82
	26–31 May 2011	342.8	7.3	394.0	0.1	−51.3	7.3	22.70	0.40	34.24	0.18	6.17	0.35	1.21	−6.09	0.63
Seasonal average		318.4	17.3	391.6	0.8	−73.2	17.4	20.99	1.30	34.17	0.39	7.20	0.30	1.16	−11.16	2.19
Summer	1–12 Jul 2009	388.7	5.0	366.7	0.2	22.0	5.0	27.12	0.27	33.95	0.14	6.75	0.12	1.14	2.76	0.63
	2–6 Jul 2007	375.0	12.5	372.9	0.2	2.1	12.5	28.24	0.29	33.76	0.12	6.95	0.25	1.27	0.35	2.07
	6–29 Aug 2008	392.7	2.4	374.7	0.2	18.1	2.4	28.70	0.23	33.48	0.17	5.51	0.16	1.18	1.63	0.21
	17–31 Aug 2009	400.4	5.8	361.0	0.3	39.4	5.8	29.49	0.25	33.66	0.13	6.05	0.23	1.47	6.68	2.10
	1–19 Jun 2011	345.1	9.8	386.6	1.2	−41.5	9.9	22.94	0.66	34.18	0.25	7.33	0.24	1.17	−6.50	0.18
	Seasonal average		380.4	8.9	372.4	0.6	8.0	8.9	27.30	0.42	33.81	0.19	6.52	0.23	1.25	0.98
Fall	18–25 Sep 2006	–	–	–	–	–	–	–	–	–	–	6.39	0.42	1.26	–	–
	14–18 Oct 2006	327.6	35.5	381.8	0.2	−54.2	35.5	25.71	0.25	34.18	0.33	7.56	0.28	1.10	−7.94	0.13
	20–24 Nov 2006	–	–	–	–	–	–	–	–	–	–	7.06	0.14	1.18	–	–
	1–10 Nov 2007	–	–	–	–	–	–	–	–	–	–	10.37	0.53	1.08	–	–
	26–30 Nov 2010	336.4	2.4	386.8	0.3	−50.4	2.4	21.84	0.24	34.42	0.04	8.39	0.40	1.11	−9.33	0.45
	Seasonal average		336.4	2.4	386.8	0.3	−50.4	2.4	21.84	0.24	34.42	0.04	8.05	0.40	1.15	−9.33
Annual average		344.0	11.7	384.7	0.7	−40.7	11.7	22.51	0.91	34.18	0.29	7.66	0.37	1.18	−7.51	1.74

[Title Page](#)
[Abstract](#)
[Introduction](#)
[Conclusions](#)
[References](#)
[Tables](#)
[Figures](#)
[◀](#)
[▶](#)
[◀](#)
[▶](#)
[Back](#)
[Close](#)
[Full Screen / Esc](#)
[Printer-friendly Version](#)
[Interactive Discussion](#)


Table 7. Data summary of Domain V. Atm. $p\text{CO}_2$ is atmospheric $p\text{CO}_2$; SST is sea surface temperature; SSS is sea surface salinity; F_{CO_2} is the air–sea CO₂ flux; SD is its standard deviation. C_2 is the nonlinearity effect of the short-term variability of wind speeds over a month on the gas transfer velocity, assuming long-term winds followed a Raleigh (Weibull) distribution (Wanninkhof, 1992; Jiang et al., 2008). See text for details. October 2006 and December 2010 were excluded in the calculations of seasonal averages. $p\text{CO}_2$ data are corrected to the reference year 2010.

Season	Period	$p\text{CO}_2$ (μatm)		Atm. $p\text{CO}_2$ (μatm)		$\Delta p\text{CO}_2$ (μatm)		SST ($^{\circ}\text{C}$)		SSS		Wind speed (m s^{-1})		C_2	F_{CO_2} ($\text{mmol m}^{-2} \text{d}^{-1}$)		
		Mean	SD	Mean	SD	Mean	SD	Mean	SD	Mean	SD	Mean	SD	Mean	Mean	SD	
Winter	23–31 Dec 2008	340.5	4.3	386.5	0.5	−46.0	4.36	21.15	0.92	34.00	0.17	9.21	0.52	1.14	−10.87	1.02	
	4–31 Dec 2009	340.8	2.9	387.3	0.3	−46.5	2.92	23.12	0.26	34.66	0.06	8.74	0.44	1.16	−10.15	0.00	
	1–3 Jan 2006	–	–	–	–	–	–	–	–	–	–	–	9.30	0.46	1.11	–	
	1–14 Jan 2009	–	–	–	–	–	–	–	–	–	–	–	10.02	0.49	1.09	–	
	1–5 Jan 2010	349.6	11.2	389.3	0.2	−39.7	11.21	20.95	1.09	34.58	0.04	8.78	0.50	1.17	−8.95	2.50	
	1–6 Feb 2010	–	–	–	–	–	–	–	–	–	–	–	8.39	0.80	1.20	–	
	1–11 Dec 2010	–	–	–	–	–	–	–	–	–	–	–	8.41	0.49	1.24	–	
	Seasonal average	343.6	8.7	387.7	0.5	−44.1	8.75	21.74	1.02	34.41	0.13	9.07	0.60	1.16	−9.99	1.91	
	Spring	15–31 Mar 2009	326.5	20.6	386.7	1.0	−60.3	20.61	24.24	1.81	34.21	0.09	8.82	0.56	1.12	−12.48	4.26
		20–30 Apr 2008	–	–	–	–	–	–	–	–	–	–	–	6.96	0.47	1.17	–
4–30 Apr 2009		354.9	6.4	387.8	1.6	−32.9	6.59	24.91	2.23	34.32	0.06	8.03	0.32	1.12	−5.63	1.09	
6–10 Apr 2009		–	–	–	–	–	–	–	–	–	–	–	8.03	0.32	1.12	–	
12–15 Apr 2011		339.8	7.0	392.5	1.0	−52.7	7.08	24.10	0.81	34.70	0.06	6.88	0.33	1.17	−7.23	−7.23	
1–20 May 2009		342.8	7.6	385.3	0.9	−42.5	7.70	24.04	1.15	34.27	0.08	6.09	0.27	1.14	−4.35	0.94	
26–31 May 2011		362.0	6.0	394.0	0.1	−32.1	6.04	24.58	0.74	34.22	0.11	6.46	0.33	1.21	−4.16	0.38	
Seasonal average		345.2	12.3	389.3	1.2	−44.1	12.39	24.37	1.64	34.34	0.09	7.32	0.41	1.15	−6.77	4.26	
Summer	1–12 Jul 2009	380.5	12.9	366.5	0.5	14.0	12.96	27.61	0.97	34.00	0.20	6.52	0.43	1.23	1.91	0.15	
	2–6 Jul 2007	388.5	11.6	373.9	1.6	14.7	11.67	28.36	1.79	34.18	0.28	6.14	0.64	1.26	1.87	0.21	
	6–29 Aug 2008	374.3	10.2	374.4	0.4	−0.1	10.23	28.64	0.39	33.05	0.33	5.33	0.31	1.24	−0.01	0.19	
	17–31 Aug 2009	378.8	19.8	363.7	0.7	15.0	19.80	28.12	0.72	33.53	0.22	5.91	0.43	1.70	3.24	4.83	
	1–19 Jun 2011	–	–	–	–	–	–	–	–	–	–	6.90	0.55	1.19	0.00	0.00	
	Seasonal average	380.5	16.3	369.6	1.1	10.9	16.34	28.18	1.27	33.69	0.30	6.16	0.54	1.32	1.75	2.79	
Fall	18–25 Sep 2006	–	–	–	–	–	–	–	–	–	–	–	6.93	0.60	1.19	–	
	14–18 Oct 2006	–	–	–	–	–	–	–	–	–	–	–	7.80	0.52	1.09	–	
	20–24 Nov 2006	–	–	–	–	–	–	–	–	–	–	–	7.27	0.38	1.16	–	
	1–10 Nov 2007	–	–	–	–	–	–	–	–	–	–	–	11.42	0.66	1.06	–	
	26–30 Nov 2010	347.9	6.1	385.9	0.6	−38.1	6.16	24.60	0.80	34.43	0.07	9.46	0.75	1.08	−8.42	2.02	
	Seasonal average	347.9	6.1	385.9	0.6	−38.1	6.16	24.60	0.80	34.43	0.07	8.77	0.75	1.12	−8.42	2.02	
Annual average	354.3	13.3	383.1	1.0	−28.8	13.35	24.72	1.41	34.22	0.20	7.83	0.68	1.19	−5.86	3.35		

Table 8. Comparison of air–sea CO₂ fluxes in the East China Sea shelf.

Study area	Season	Methods ^a	Wind speed	k ^b	FCO ₂ (mmol m ⁻² d ⁻¹)	FCO ₂ -S(07) ^c (mmol m ⁻² d ⁻¹)	Data source
Domain I	Spring	1	Short-term	W92_S	-8.8 ± 5.8	-7.7 ± 5.1	Zhai and Dai (2009)
	Spring	1	Monthly	S07	-10.7 ± 8.2	-10.7 ± 8.2	This study
	Summer	1	Short-term	W92_S	-4.9 ± 4.0	-4.3 ± 3.5	Zhai and Dai (2009)
	Summer	1	Monthly	S07	-6.5 ± 10.7	-6.5 ± 10.7	This study
	Fall	1	Short-term	W92_S	2.9 ± 2.5	2.5 ± 2.2	Zhai and Dai (2009)
	Fall	1	Monthly	S07	2.2 ± 6.8	2.2 ± 6.8	This study
	Winter	1	Short-term	W92_S	-10.4 ± 2.3	-9.1 ± 2.0	Zhai and Dai (2009)
	Winter	1	Monthly	S07	-9.8 ± 4.6	-9.8 ± 4.6	This study
	Annual	1	Short-term	W92_S	-5.2 ± 3.6	-4.5 ± 3.1	Zhai and Dai (2009)
	Annual	1	Monthly	S07	-6.2 ± 9.1	-6.2 ± 9.1	This study
Domains I and III	Spring	1	Monthly	W92_L	-5.0 ± 1.6	-4.2 ± 1.3	Shim et al. (2007)
	Spring	1	Daily	W92_S	-6.8 ± 4.3	-5.9 ± 3.7	Kim et al. (2013)
	Spring	1	Monthly	S07	-	-13.0 ± 6.6	This study
	Summer	1	Daily	W92_S	-6.6 ± 8.5	-5.7 ± 7.4	Kim et al. (2013)
	Summer	1	Monthly	S07	-	-5.8 ± 8.5	This study
	Fall	1	Monthly	W92_L	1.1 ± 2.9	0.9 ± 2.4	Shim et al. (2007)
	Fall	1	Daily	W92_S	0.8 ± 7.3	0.7 ± 6.4	Kim et al. (2013)
	Fall	1	Monthly	S07	-	0.2 ± 6.2	This study
	Winter	1	Daily	W92_S	-12 ± 4.1	-10.5 ± 3.6	Kim et al. (2013)
	Winter	1	Monthly	S07	-	-10.1 ± 3.6	This study
	Annual	4	-	-	-8	-	Tsunogai et al. (1999)
	Annual	1	Daily	W92_S	-6.0 ± 5.8	-5.2 ± 5.0	Kim et al. (2013)
	Annual	1	Monthly	S07	-	-7.2 ± 6.2	This study
	Domains I, III and IV	Summer	2	-	L&M86; T90	-1.8 to -4.8	-
Summer		1	Monthly	S07	-	-4.6 ± 5.9	This study
Domains II, IV and V	Spring	2	Long-term	-	-5.8 ± 7.7	-	Peng et al. (1999)
	Spring	1	Monthly	S07	-	-9.5 ± 2.0	This study
ECS shelf	Spring	3	Monthly	S07	-	-8.2 ± 2.1	Tseng et al. (2014)
	Spring	3	Long-term	W92_L	-11.5 ± 2.5	-9.6 ± 2.1	Tseng et al. (2011)
	Spring	1	Monthly	S07	-	-11.7 ± 3.6	This study
	Summer	1	Daily	S07	-	-2.4 ± 3.1	Chou et al. (2009a)
	Summer	3	Long-term	W92_L	-1.9 ± 1.4	-1.6 ± 1.2	Tseng et al. (2011)
	Summer	3	Monthly	S07	-	-2.5 ± 3.0	Tseng et al. (2014)
	Summer	1	Monthly	S07	-	-3.5 ± 4.6	This study
	Fall	3	Long-term	W92_L	-2.2 ± 3.0	-1.8 ± 2.5	Tseng et al. (2011)
	Fall	3	Monthly	S07	-	-0.8 ± 1.9	Tseng et al. (2014)
	Fall	1	Monthly	S07	-	-2.3 ± 3.1	This study
	Winter	1	Monthly	W92_L	-13.7 ± 5.7	-11.4 ± 4.7	Chou et al. (2011)
	Winter	3	Long-term	W92_L	-9.3 ± 1.9	-7.7 ± 1.6	Tseng et al. (2011)
	Winter	3	Monthly	S07	-	-5.5 ± 1.6	Tseng et al. (2014)
	Winter	1	Monthly	S07	-	-10.0 ± 2.0	This study
	Annual	3	Long-term	W92_L	-6.3 ± 1.1	-5.2 ± 0.9	Tseng et al. (2011)
	Annual	3	Monthly	S07	-	-3.8 ± 1.1	Tseng et al. (2014)
	Annual	1	Monthly	S07	-	-6.9 ± 4.0	This study

^a Methods

- 1: pCO₂ measurements and gas transfer algorithms with wind speeds;
- 2: pCO₂ calculated from DIC and TA and gas transfer algorithms with wind speeds;
- 3: pCO₂ algorithms (with Changjiang discharge and SST) and gas transfer algorithms with wind speeds;
- 4: pCO₂ measurements and algorithms (with SST, SSS and phosphate) and given gas transfer velocity;

^b: W92_S is Wanninkhof (1992) algorithm for short-term wind speeds; W92_L is Wanninkhof (1992) algorithm for long-term (or monthly average) wind speeds; S07 is Sweeney et al. (2007) algorithm; L&M86 is Liss and Merlivat (1986) algorithm; T90 is Tans (1990) algorithm.

^c: FCO₂ data were calculated (or recalculated) with the Sweeney et al. (2007) gas transfer algorithm with wind speed.

BGD

12, 5123–5167, 2015

Air–sea CO₂ fluxes in the East China Sea

X.-H. Guo et al.

Title Page

Abstract

Introduction

Conclusions

References

Tables

Figures

◀

▶

◀

▶

Back

Close

Full Screen / Esc

Printer-friendly Version

Interactive Discussion



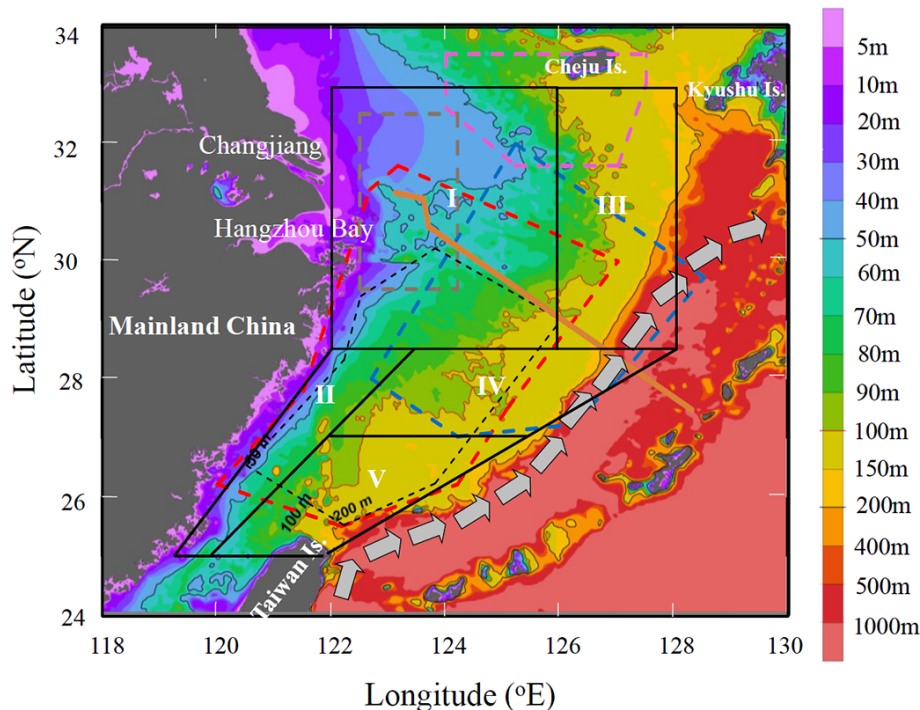


Figure 1. Map of the East China Sea showing the study area. Areas framed with black solid lines indicate the five physico-biogegeochemical domains categorized in this study to better constrain the spatial and temporal variability of CO₂ fluxes, as detailed in Table 1. The arrows show the direction of the Kuroshio Current. The area framed by pink dashed lines shows the study area of Shim et al. (2007) and Kim et al. (2013); by brown dashed lines of Zhai and Dai (2009); by blue dashed lines of Wang et al. (2000); by red dashed lines of Chou et al. (2009a, 2011) and Tseng et al. (2011); and by black dashed lines of Peng et al. (1999). The solid brown line is the PN line which was the major survey track of Tsunogai et al. (1999).

Title Page

Abstract

Introduction

Conclusions

References

Tables

Figures

◀

▶

◀

▶

Back

Close

Full Screen / Esc

Printer-friendly Version

Interactive Discussion



Air–sea CO₂ fluxes in
the East China Sea

X.-H. Guo et al.

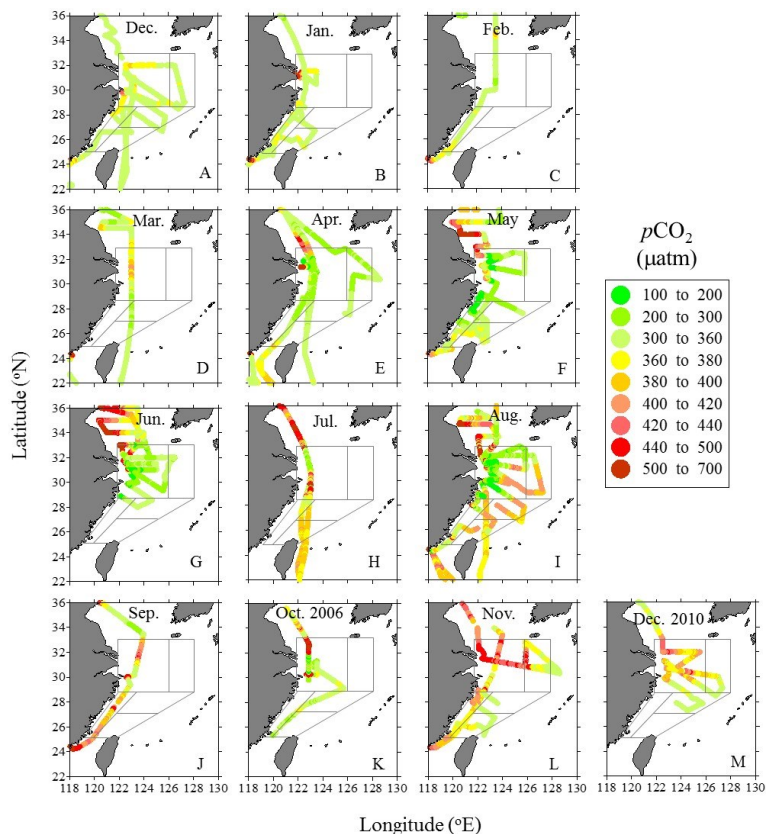


Figure 2. Spatial distribution of surface water $p\text{CO}_2$ (μatm) in the East China Sea in the 12 month surveys of 2006 to 2011. The framed areas show the five physico-biogeochemical domains. Data are corrected to the reference year 2010.

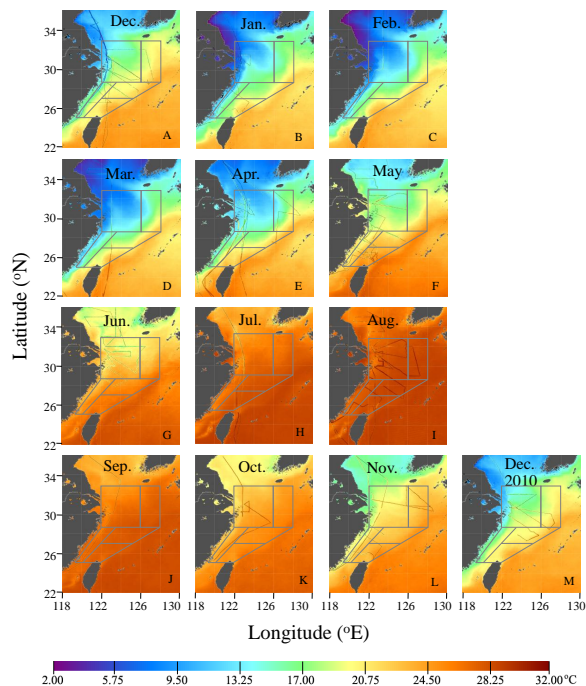


Figure 3. Spatial distribution of sea surface temperature (SST) in the East China Sea in the 12 month surveys of 2006 to 2011. The climatology (from 2003 to 2013) monthly-mean SST were calculated based on the monthly mean SST obtained from the NASA ocean color website (<http://oceancolor.gsfc.nasa.gov>), which were retrieved with the Moderate Resolution Imaging Spectroradiometer (MODIS) on board the Aqua satellite. The 4 μm nighttime SST products were used here. The SST data in the track were measured during the surveys. The framed areas show the five physico-biogeochemical domains. In panel M, the SST data in the track were measured during the December 2010 cruise while the background is the climatology (from 2003 to 2013) monthly-mean SST.

Title Page

Abstract

Introduction

Conclusions

References

Tables

Figures



Back

Close

Full Screen / Esc

Printer-friendly Version

Interactive Discussion



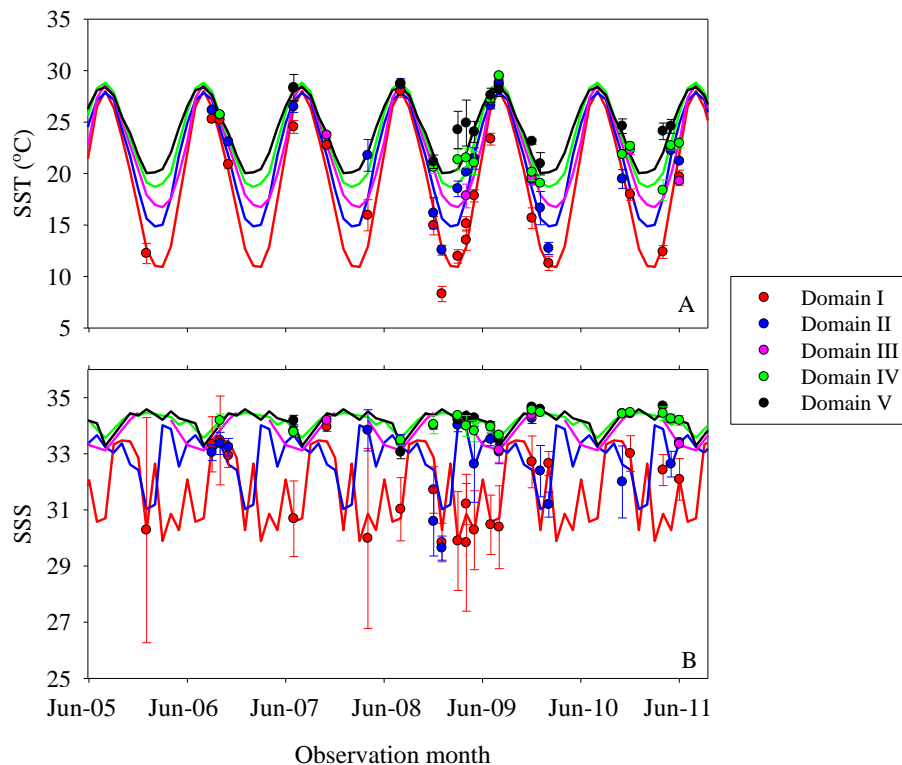


Figure 4. Seasonal variations of sea surface temperature (SST, **a**) and salinity (SSS, **b**) in Domain I (red curve), Domain II (blue curve), Domain III (pink curve), Domain IV (green curve) and Domain V (black curve). The mean SST data were retrieved with the Moderate Resolution Imaging Spectroradiometer (MODIS) on board the Aqua satellite from NASA ocean color website (<http://oceancolor.gsfc.nasa.gov>). The $4\ \mu\text{m}$ nighttime SST products were used here. The mean SSS were based on the data presented in Tables 3–7. The data during each survey are shown as mean \pm SD.

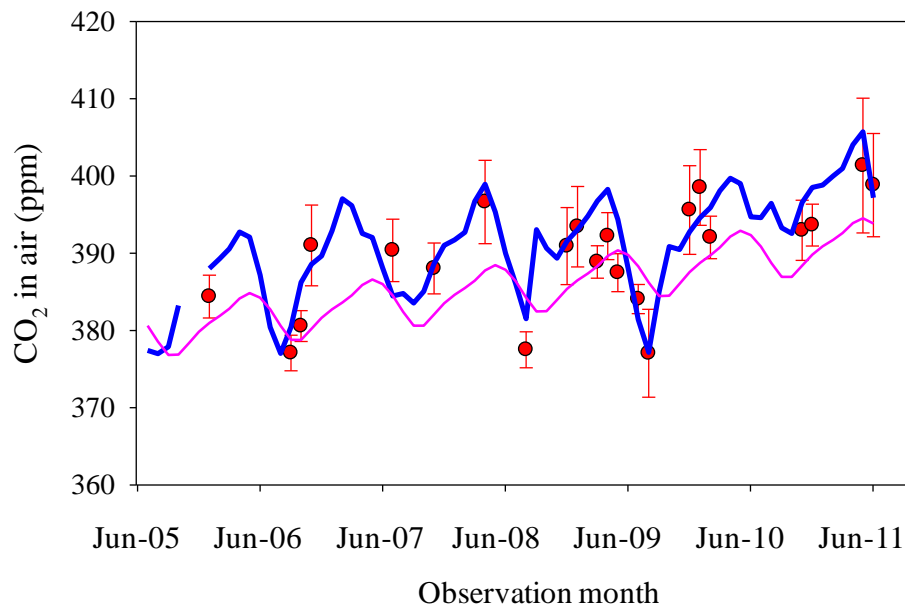


Figure 5. Temporal distribution of atmospheric CO₂ concentrations based on ship-board measurements during the cruise to the East China Sea (arithmetic average, red solid dots) and its comparison with the measurements at 21 m.a.s.l., at Tae-ahn Peninsula (blue solid line) (36.7376° N, 126.1328° E, Republic of Korea, <http://www.esrl.noaa.gov/gmd/dv/site>) and at Mauna Loa Observatory at Hawaii (pink solid line, Scripps CO₂ program, <http://scrippsco2.ucsd.edu>). The error bars are the SDs. The CO₂ concentrations in this plot are the original values in the year of the observations.



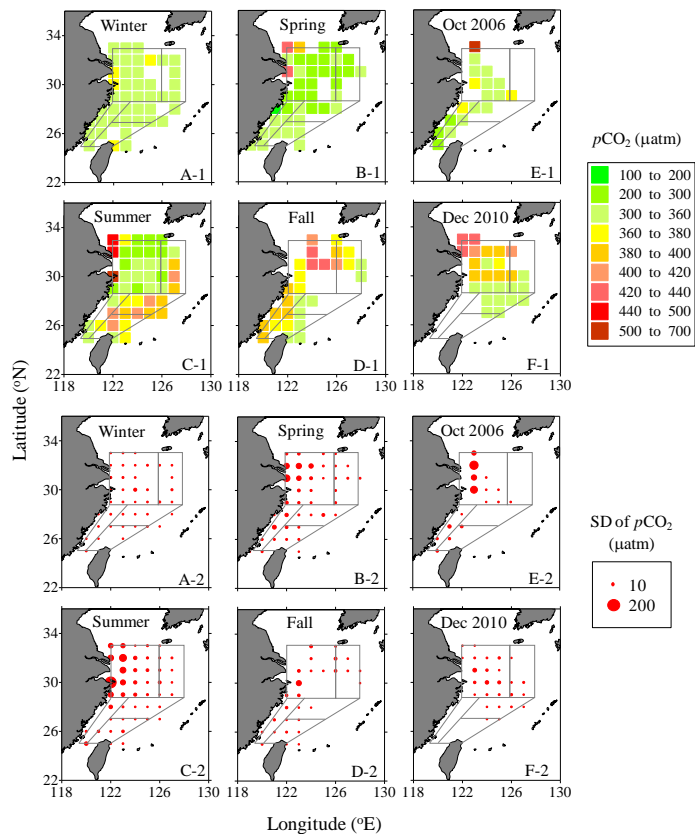


Figure 6. Distribution of seasonal average and SDs of $p\text{CO}_2$ in $1^\circ \times 1^\circ$ grids on the East China Sea shelf. The framed areas show the five physico-biogeochemical domains. **(a-1)** and **(a-2)** are the result of the winter cruises excluding December 2010; **(d-1)** and **(d-2)** are results of the fall cruises excluding October 2006. Data are corrected to the reference year 2010.

Air–sea CO₂ fluxes in the East China Sea

X.-H. Guo et al.

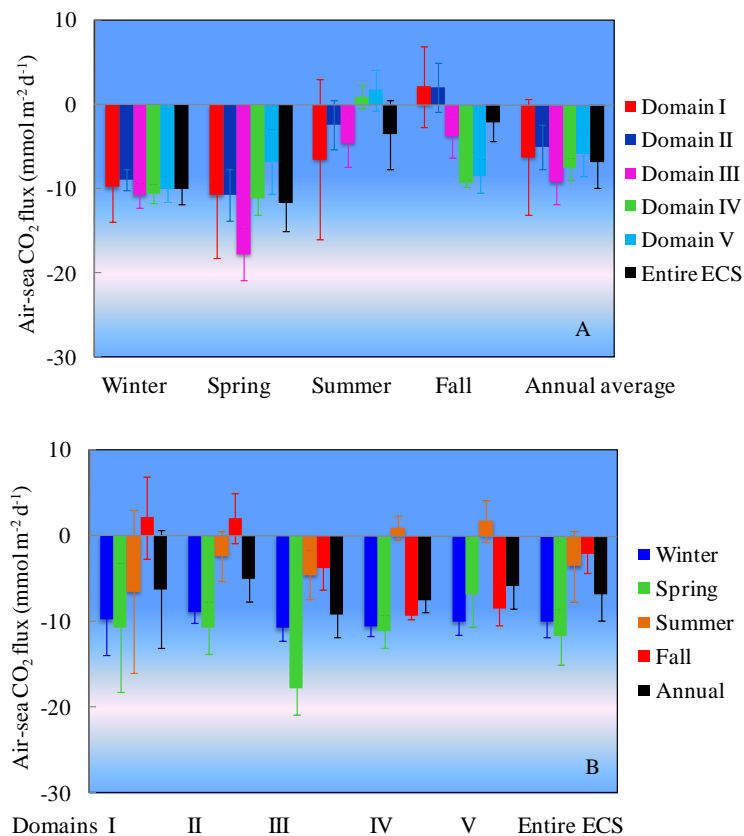


Figure 7. CO₂ fluxes and seasonal variations in the East China Sea. The error bars are the SDs.

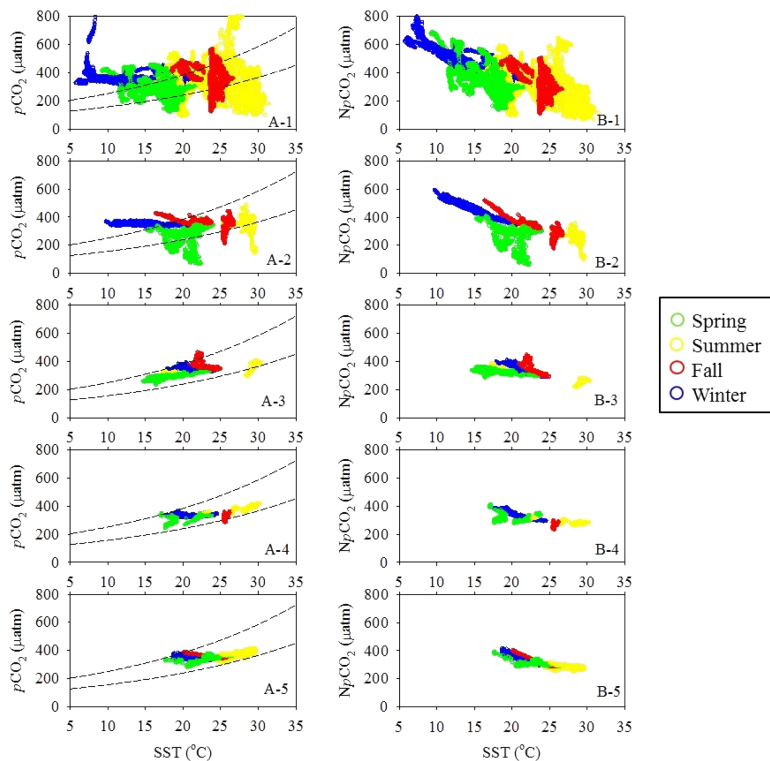


Figure 8. Relationships of $p\text{CO}_2$ and $Np\text{CO}_2$ (normalized $p\text{CO}_2$ to 21°C) of the surface water with sea surface temperature (SST). **(a-1)** and **(b-1)** are Domain I; **(a-2)** and **(b-2)** are Domain II; **(a-3)** and **(b-3)** are Domain III; **(a-4)** and **(b-4)** are Domain IV; **(a-5)** and **(b-5)** are Domain V. The dashed lines in **(a-1)** to **(a-5)** represent $250 \times \exp((\text{SST} - 21) \times 0.0423)$ and $400 \times \exp((\text{SST} - 21) \times 0.0423)$ μatm , in which 250 and 400 μatm are the lower and higher limits of $Np\text{CO}_2$ in Domains IV and V (see details in the text). $p\text{CO}_2$ and $Np\text{CO}_2$ values are in the year of observations.

Title Page

Abstract

Introduction

Conclusions

References

Tables

Figures

I ◀

▶ I

◀

▶

Back

Close

Full Screen / Esc

Printer-friendly Version

Interactive Discussion



Air–sea CO₂ fluxes in
the East China Sea

X.-H. Guo et al.

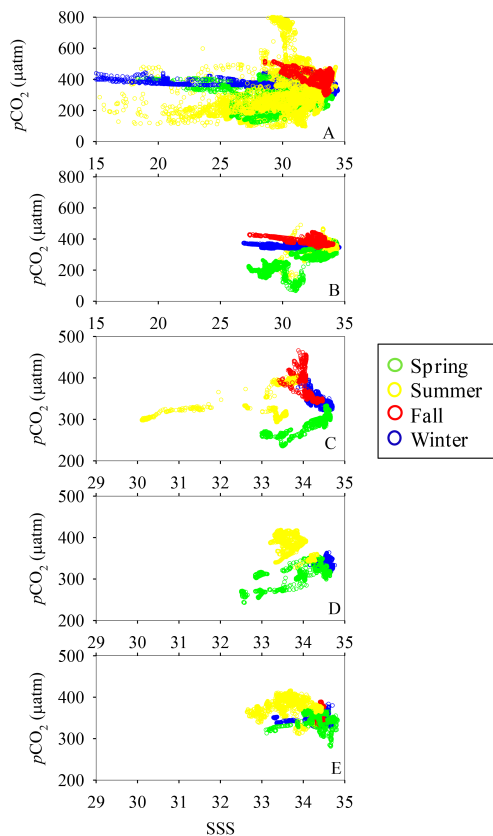


Figure 9. Relationships of $p\text{CO}_2$ of the surface water with sea surface salinity (SSS). (a–e) are Domains I to V, respectively. $p\text{CO}_2$ values are in the year of observations.

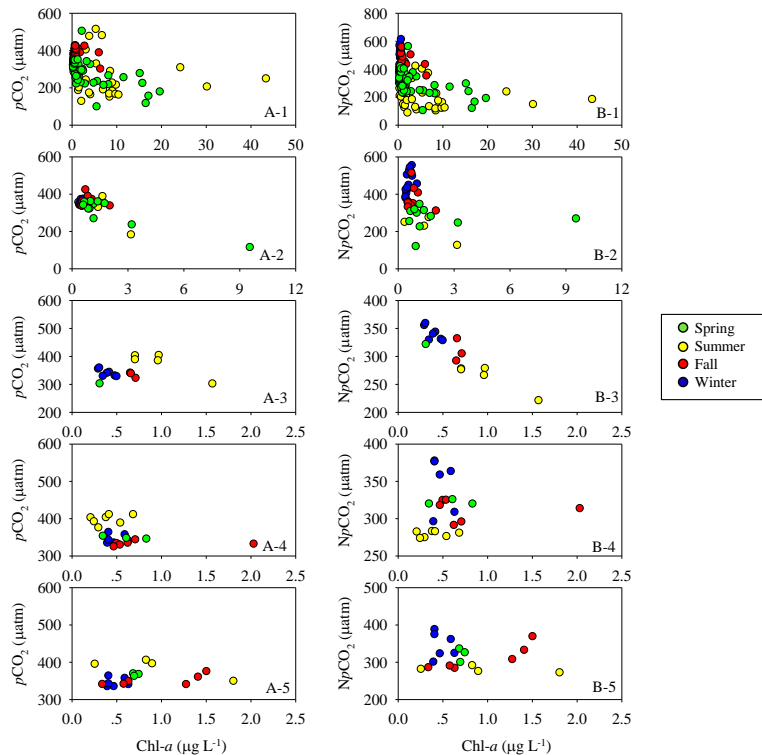


Figure 10. Relationships of $p\text{CO}_2$ and $Np\text{CO}_2$ (normalized $p\text{CO}_2$ to 21°C) with chlorophyll *a* (*chl a*) concentration. The data of *chl a* concentration in surface water were unpublished data from Dr. Jun Sun. The spring surveys include April and May 2011; the summer surveys include July and August 2009; the fall surveys include November 2010; and the winter surveys include December 2009 and January 2010 surveys. **(a-1)** and **(b-1)** are Domain I; panels **(a-2)** and **(b-2)** are Domain II; **(a-3)** and **(b-3)** are Domain III; panels **(a-4)** and **(b-4)** are Domain IV; panels **(a-5)** and **(b-5)** are Domain V. $p\text{CO}_2$ and $Np\text{CO}_2$ values are in the year of observations.